

Translational Profiling Reveals Temporal Dynamics of
Dendritic Protein Synthesis

A thesis submitted by

Alexander Jones

in partial fulfillment of the requirements for the degree of

PhD

In

Neuroscience

Tufts University

Sackler School of Graduate Biomedical Sciences

February 2019

Advisor: Leon Reijmers, PhD

Abstract

It is well established that the long term storage of new memories requires on demand synthesis of new proteins in the minutes and hours following that memories formation. This requirement is specific to discrete subcellular compartments. Specifically, neuronal dendrites synthesize new proteins locally and disruption of this process impairs synaptic plasticity and long-term memory in hippocampal slice experiments and *in vivo* behavioral experiments, respectively. Although recent studies have attempted to determine the translational profile of dendrites within the hippocampus, no current consensus exists. Furthermore, it is not known how this translational profile changes during the course of memory consolidation. Understanding the dynamics of protein translation in dendrites is an important step in understanding why this process is necessary for memory.

Using a previously generated mouse line, which expresses an EGFP-tagged ribosomal subunit under the control of the *Camk2a* promoter, we isolated ribosome bound mRNA from dendrites and somata of projection neurons in CA1 of the hippocampus. In a previous study we successfully used this technique combined with RNAseq to generate a list of likely-dendritic mRNAs. Here we update this list, considerably expanding the sample size used to generate our predictions. We find that our updated list of dendritic predictions overlaps with some, though not all, of the genes previously predicted to be dendritic. We compared mRNAs that are predicted to be bound preferentially to ribosomes in dendrites versus in somata and found differences in the untranslated regions of these genes underscoring the ability for elements of the

untranslated region to act as localization signals that target these genes to distinct subcellular compartments.

We further explored the translational profile of dendrites and somata during the early time course after a behavioral learning paradigm. We find that mRNAs in dendrites in particular experience an early and late phase of ribosome binding increases as compared with mice that did not undergo a learning paradigm. These separate phases of ribosome binding constitute a pool of mRNAs that are involved in functionally distinct biological processes. Furthermore, the translational profiles of dendrites and somata are almost entirely non-overlapping underscoring the point that changes in protein synthesis during memory are subcellular compartment specific. The temporal pattern of these phases of ribosome binding provides new insight into how local translation within dendrites might be regulated in response to learning. We hope that in addition, our results will be a resource to the field of local dendritic translation.

Table of contents

Title Page.....	i
Abstract.....	ii
Table of contents.....	iv
List of tables.....	vi
List of figures.....	vii
List of abbreviations.....	viii
Chapter 1: Introduction.....	1
1.1 Protein Synthesis and Memory.....	2
1.1.1 Protein synthesis is required for long-term memory.....	2
1.1.2 Regulation of protein synthesis in memory.....	3
1.2 Local Protein Synthesis.....	7
1.2.1 Support for local protein synthesis in dendrites.....	7
1.2.2 Localization of mRNAs into dendrites.....	9
1.3 Gene Expression Profiling and Memory.....	11
1.3.1 Next generation tools for studying protein synthesis in memory.....	12
1.3.2 Recent translational profiling studies of protein synthesis during memory..	17
1.4 Contributions of this Thesis.....	18
Chapter 2: Methodology.....	20
2.1 Animals.....	21
2.2 Fear Conditioning.....	21
2.3 mRNA Isolation and Immunoprecipitation.....	22
2.4 Quantitative RT-PCR and Bioanalyzer Analysis.....	24
2.5 Library preparation and RNA-sequencing.....	25
2.6 Tissue preparation and immunohistochemistry.....	26
2.7 Microscopy.....	27
2.8 Statistical analysis.....	28
Chapter 3: Results.....	29
3.1 Diverse pools of mRNAs localize to discrete neuronal compartments.....	30
3.1.1 Isolation of mRNA from CA1 projection neuron dendrites and somata.....	30
3.1.2 Translational profiling of discrete subcellular compartments of CA1 Projection neurons.....	35
3.1.3 Differences in regulatory elements of mRNAs enriched in dendrites or somata.....	41

3.1.4 Prediction of dendritically localized mRNAs.....	43
3.2 Divergent temporal dynamics of neuronal compartments after contextual fear conditioning.....	45
3.2.1 TRAP greatly enhances detection of translational changes in dendrites and somata.....	48
3.2.2 Temporal patterns of alteration in ribosome binding in dendrites and somata.....	49
3.2.3 Early and intermediate ribosome binding engage alternate functions in dendrites.....	52
Chapter 4: Discussion.....	58
4.1 Translational profiling of dendritic and somatically localized mRNAs.....	59
4.1.1 Prediction of dendritic mRNAs, past and present.....	59
4.1.2 Implications of dendritic mRNA diversity for synaptic plasticity mechanisms.....	61
4.1.3 Regulatory features associated with Dendritic mRNAs.....	64
4.2 Temporal dynamics of protein translation during memory.....	68
4.2.1 Advantages of TRAP for studying changes in local translation over time...	68
4.2.2 Multiple waves of protein synthesis in dendrites after learning.....	72
4.3 Future Directions.....	75
4.4 Concluding remarks.....	77
Chapter 5: References.....	78

List of tables

Table 2.1: qPCR primer sequences..... 25

List of figures

Figure 3.1: Collection of dendritic and somatic mRNA by TRAP.....	33
Figure 3.2 RNA-seq confirms specificity of TRAP mRNA collection.....	37
Figure 3.3 Differential expression analysis reveals greater diversity of ribosome-bound mRNAs in dendrites than somata.....	40
Figure 3.4 Ribosome-bound genes in dendrites and somata display alternate trends in UTR length and enrichment of certain regulatory features.....	44
Figure 3.5 Logistic regression analysis predicts dendritically localized genes.....	46
Figure 3.6 TRAP improves differential expression analysis of fear conditioning Time-course.....	51
Figure 3.7 Temporal patterns of differential expressed genes in dendrite IP.....	53
Figure 3.8 Temporal patterns of differential expressed genes in soma IP.....	54
Figure 3.9 Temporally derived gene clusters are functionally distinct.....	56

List of abbreviations

BDNF:	Brain-derived neurotrophic factor
CA1:	Cornus ammonis region 1 of the hippocampus
CA3:	Cornus ammonis region 3 of the hippocampus
Camk2a:	Calcium/calmodulin-dependent protein kinase II alpha
CREB:	cAMP response element-binding protein
dCt:	Delta cycle threshold
DE:	Differentially expressed
EGFP:	Enhanced green fluorescent protein
EGFP-L10a:	Enhanced green fluorescent protein fused to the RPL10a subunit
ERK:	Extracellular signal-regulated kinase
FACS:	Fluorescence-activated cell sorting
FC:	Fear conditioned
FC0:	Fear conditioned, 0 minute delay before dissection
FC15:	Fear conditioned, 15 minute delay before dissection
FC30:	Fear conditioned, 30 minute delay before dissection
FMRP:	Fragile X mental retardation protein
FPKM:	Fragments per kilobase of transcript per million mapped reads
Gfap:	Glial fibrillary acidic protein
GFP:	Green fluorescent protein
GO:	Gene ontology
HC:	Home cage
IEG:	Immediate early gene
IP:	Immunopurification
LCM:	Laser capture microdissection
LTD:	Long-term depression
LTP:	Long-term potentiation
MAPK:	Mitogen-activated protein kinase
mGluR:	Metabotropic glutamate receptor
mRNA:	Messenger ribonucleic acid
mTOR:	Mammalian target of rapamycin
NMDA:	N-Methyl-D-aspartate
qPCR:	Quantitative real-time polymerase chain reaction
RIN:	Ribonucleic acid integrity number
Rps15a:	Small ribosomal protein S15a
RPL9:	Large ribosomal protein L9
RPL18:	Large ribosomal protein L18
rRNA:	Ribosomal ribonucleic acid
SN:	Supernatant
tetO:	Tetracycline operator
TOP:	5' Terminal oligopyrimidine motif
TRAP:	Translating ribosome affinity purification

tTA: Tetracycline-transactivator
uORF: Upstream open reading frame
UTR: Untranslated region

Chapter 1: Introduction

The ability to encode and store memories is arguably the most important function of the central nervous system. How this phenomenon occurs, in which experience is captured by complex chemical and physical changes in the brain, has been a central question in neuroscience since Santiago Ramon y Cajal first suggested that learning was the result of changes in synaptic strength[1]. The development of behavioral models and a slew of new tools has since allowed us to directly probe the mechanisms of memory storage.

1.1 Protein Synthesis and Memory

1.1.1 Protein synthesis is required for long-term memory

During the mid-1900's, a growing sense that protein synthesis was somehow linked to memory storage was finally made testable by the discovery of the protein synthesis inhibiting drug, puromycin [2]. In 1963, Josefa Flexner et al. showed that intracranial injection of puromycin into the temporal lobe could block memory formation in mice [3]. Mice that had received injections of puromycin in the first three days following a behavioral task in which they learned the location an electric shock would be delivered were later unable to recall this memory. Injections made after three days did not result in a memory deficit, indicating that there is a critical period for memory formation during which protein synthesis is required. In the decades since it has become clear that while memory acquisition and short term memory storage during the minutes to hours after a memory is formed are independent of protein synthesis, the long term storage of those memories requires it [4].

The use of protein synthesis inhibiting drugs came with several drawbacks. For one, exact placement and spread of the drug within a brain region was difficult to control. For another, these drugs could not differentiate between constitutive protein synthesis and that which was initiated during the formation of a memory. The use of these drugs thus gradually gave way to more precise genetic manipulations. In 2004 Raymond Kelleher et al. noted that the ERK/MAPK pathway, which was known to be involved in synaptic activity and plasticity, may also be involved in regulation of protein translation. By expressing a dominant negative form of the ERK kinase, MEK1, specifically in Camk2a-expressing neurons of the mouse forebrain, they were able to show that loss of this signalling pathway produced memory and plasticity deficits and that those deficits were coupled with loss of translational regulation in those neurons [5]. In another study Mauro Costa-Mattioli et al. showed that knockout of the protein kinase GCN2, which stimulates the translation of ATF4, a CREB antagonist, lead to dysregulation of both long term potentiation and memory[6].

1.1.2 Regulation of protein synthesis in memory

An important corollary of the research showing the need for protein synthesis during memory formation is that not only constitutive protein synthesis is required. Indeed as the studies from Kelleher and Costa Mattioli suggested, interfering with the activation of specific signaling pathways and the downstream translational regulation they employ is sufficient to cause deficits in long term memory storage. The complex signaling mechanisms through which neurons are activated during plasticity and long

term memory may ultimately comprise many overlapping modes of translational regulation. Fortunately, much work has been done describing the various means by which protein synthesis may be regulated during memory [7].

In eukaryotes, initiation appears to be the most common rate limiting step in translating a given mRNA. Initiation is the formation of the complete ribosomal complex at the 5' end of the mRNA transcript. This is accomplished in a stepwise fashion whereby, the small 40S ribosomal subunit is first assembled into a pre-initiation complex, followed by the association of the mRNA with the preinitiation complex and finally assembly of the full 80s ribosomal complex. This process can be regulated at two key points. First, phosphorylation at Ser51 of the eukaryotic initiation factor eIF2a inhibits the exchange of GDP for GTP on the preinitiation complex, which results in its not being incorporated into the preinitiation complex and a subsequent downregulation of translation [8]. GCN2, the only eIF2a kinase conserved from yeast to mammals [9] regulates this process. As mentioned above, the activity of this kinase stimulates the synthesis of ATF4. This counter intuitive process is accomplished thanks to a secondary effect of eIF2a phosphorylation which leads to an increase in translation for a subset of mRNAs that contain upstream open reading frames (uORFs) within their 5'UTRs [10]. Approximately 40 percent of all mammalian genes are estimated to contain at least one uORF [11] making this an important potential mechanism of translational regulation.

The second major point of regulation during initiation is the loading of the mRNA onto the preinitiation complex. The best characterized mode of regulation of this process is mediated via the mammalian target of rapamycin or mTOR. mTOR is a kinase which is

responsible for, among other things, phosphorylating eIF4E binding proteins (4E-BPs) which inhibit protein synthesis by preventing eIF4E from being assembled into the eIF4F complex and thus preventing loading of ribosomes on mRNA [12,13]. In particular, the mTOR complex mTORC1 almost exclusively regulates the translation of mRNAs containing a 5' terminal oligopyrimidine (TOP) motif. In a recent study, Carson Thoreen et al. definitively showed that the selectivity of mTORC1 for regulation of TOP motif containing mRNAs worked through its interactions with 4E-BPs rather than some other mechanism as had been suspected [14]. There is substantial evidence that mTOR signaling by the ERK pathway is important, in particular, in the hippocampus where downstream mTOR effectors generally activated by numerous stimulation paradigms can be blocked by ERK inhibitors [15–17].

The engagement of the molecular mechanisms governing translation is not limited to any single modality of synaptic plasticity. In fact, both enhancements of synaptic strength via long-term potentiation (LTP) and decrement of synaptic strength via long-term depression (LTD) require protein synthesis for the maintenance of those modifications to synaptic strength [16,18,19]. Interestingly, the mechanisms for achieving long term plastic changes in synapse strength have been shown to overlap considerably regardless of the direction of those changes. For example, Sreedharan Sajikumar and Julietta Frey showed in 2004 that induction of late-LTD which requires protein synthesis at one synapse could induce either late-LTP or late-LTD (both of which are protein synthesis dependent) at a neighboring synapse, even in the presence of protein synthesis inhibitors [20]. Thus, a common pool of proteins are likely to be translated that can

support plastic changes in synaptic strength, and the direction of those changes is likely mediated by the nature of the upstream neuronal activity in (at least partially) a protein synthesis-independent manner. The translation of these common pools of proteins is mediated in part by molecular mechanisms that are engaged by multiple upstream processes. For example, as mentioned above, the ERK pathway is activated by numerous stimulation paradigms including both NMDA receptor activation [15] and mGluR receptor activation [21].

On the other hand, differences in protein synthesis for specific genes have been demonstrated for varying modes of synaptic plasticity. One well-studied example is the gene *Arc*, translation of which is increased at synapses in response to NMDA-mediated LTP and mGluR-mediated LTD but not NMDA-mediated LTD [22–24]. Indeed, gene specific differences in translation can be driven in response to the diverse downstream pathways that are engaged by different modes of neuronal activation. In particular, RNA binding proteins that target specific sequence motifs within mRNAs can regulate the translational status of those mRNAs. NMDA receptor activation drives the phosphorylation of cytoplasmic polyadenylation element binding protein (CPEB) which specifically regulates the translation of mRNAs containing a cytoplasmic polyadenylation elements (CPE) [25,26]. Loss of the RNA-binding protein Fragile-X Mental Retardation Protein (FMRP) leads to an enhancement of mGluR dependent late-LTD [27,28]. Thus, both general translational mechanisms (as above) and gene specific translational mechanisms are engaged during plasticity and memory, however the full extent of each of those mechanisms and how they interact with each other is not yet known [16].

Taken together, these findings paint a vivid picture. Protein synthesis in the minutes and hours following acquisition is necessary for long term storage of a memory. The synthesis of these proteins is not merely constitutive but rather is regulated by neuronal activity. And finally, multiple signalling pathways are involved in the regulation of said protein synthesis.

1.2 Local Protein Synthesis

1.2.1 Support for local protein synthesis in dendrites

As the idea that protein synthesis was required for memory was beginning to gain ground, a parallel discovery was made. Although it had been speculated that all proteins were synthesized within the cytoplasm, in 1964 David Bodian first observed the presence of ribosomal particles in close apposition with “synaptic knobs” within proximal dendrites in electron microscopy images of monkey spinal cord[29]. This placement of ribosomes it turned out, was commonplace and as Bodian suggested, was likely to have some functional relevance. Further solidifying this idea, Oswald Steward and William Levy showed that polyribosomes tended to cluster in dendritic spines of dentate granule cells, distal to the somata[30]. The distal placement of these polyribosomes ran counter to the idea that postsynaptic proteins were synthesized solely in the soma and trafficked out along the dendrite.

In the early 1990’s a series of studies added support for the idea of local protein synthesis, showing that biochemical fractions enriched for synaptoneuroosomes (synaptic fragments, sheared from the neuron during fractionation) not only contained ribosomes,

but could incorporate radiolabeled amino acids into a new polypeptide chain after fractionation [31–33]. In 1993, Sherry Feig and Peter Lipton used radiolabeled amino acids to demonstrate protein synthesis in CA1 dendrites of hippocampal slices from guinea pig [34]. This protein synthesis was dependent upon stimulation and occurred within minutes. The rapid time frame and the fact that no corresponding increase in protein synthesis was observed in soma was evidence that the increases in dendritic protein were due to local protein synthesis. More recently, dendritic protein synthesis was visualized in cultured hippocampal neurons using alternative amino acids that could be substituted for their endogenous counterparts, incorporated into newly synthesized proteins and subsequently labeled by chemical modification [35].

Functional support for the hypothesis that local protein synthesis is involved in memory was first shown by Hyejin Kang and Erin Schuman. They demonstrated that enhancements of synaptic transmission induced by the neurotrophic factor BDNF were dependent upon local translation. In rat hippocampal slices that had been lesioned to isolate CA1 dendrites from their somata, BDNF application enhanced synaptic transmission. Treatment of lesioned hippocampal slices with the protein synthesis inhibitor anisomycin blocked this enhancement [36]. Dendritic protein synthesis has since been shown to be required for a number of modalities of synaptic plasticity, including: mGluR-dependent long-term depression [19] and NMDA-dependent long term potentiation [37]. Separately, the discovery that the 3'UTR of the mRNA *Camk2a* contained a targeting element responsible for its localization into dendrites made it possible to directly test the effects of local protein synthesis on behavior *in vivo* [38].

This was elegantly done by Stephan Miller et al. using a genetic mouse model in which the *Camk2a* gene was truncated to exclude the dendritic targeting element. The truncated mRNA failed to localize to dendrites in CA1 of the hippocampus and these led to deficits in hippocampal dependent memory tasks and synaptic plasticity in these mice [39].

Together these studies established that local translation of specific proteins was required for long term memory.

As evidence for the role of local protein synthesis in memory mounted, it became obvious that questions about the specifics of this process would need to be addressed.

What is the precise timing of local translation in dendrites? Do the mRNAs exist in dendrites as a ready pool or do they require translocation from elsewhere in the neuron?

What specific set of proteins are synthesized locally and how does this translational profile respond to neural activity? What molecular mechanisms regulate local translation generally and in response to activity?

1.2.2 Localization of mRNAs into dendrites

A large body of work has gone into understanding the dynamics of RNA localization. The presence of *cis*-acting signals within an mRNA's 3'UTR can determine the localization of that mRNA. These signals are bound by various RNA binding proteins which act in *trans* in order to guide these mRNAs to their ultimate destination (reviewed in [40,41]). Truncation of the *Camk2a* 3'UTR to remove its dendritic targeting element efficiently blocked the vast majority of dendritic localization for this mRNA [38] and as was discussed above, subsequently blocked plasticity and memory [39]. This supports the

idea the Camk2a is part of a readily available pool of mRNAs that are available to be translated in dendrites and which are required for memory. However, these studies did not preclude the possibility that localization of certain mRNAs to the dendrite may be concurrent with neural activity.

Activity dependent localization of mRNAs was described in the mid 1990's by Roger Knowles et. al. In two consecutive studies, they labeled RNA granules with SYTO 14, which fluoresces on contact with nucleic acid, and measured the dynamics of those RNA granules in cultured hippocampal neurons by time-lapse imaging. RNA granules were found to move at approximately 6 $\mu\text{M}/\text{min}$. Application of the neurotrophin NT-3 onto hippocampal neurons induced the translocation of RNA granules into dendrites. Based on these findings and the average distance of CA1/CA3 dendritic fields from their cell bodies (100 - 150 μM) they estimated that upon stimulation, RNA granules could arrive at sites of synaptic activity within 30 minutes [42,43]. Further support for RNA localization directly to sites of synaptic activity was shown in 2002. Linnaea Osstroff et al. showed that tetanic stimulation of hippocampal slices from rat could induce the translocation of polyribosomes from dendritic shafts into spines. Furthermore, spines which contained polyribosomes following tetanic stimulation contained larger post-synaptic densities, indicating structural plasticity may be linked to local translation [44].

There are thus two potential pools of mRNA from which neuronal dendrites might draw: a ready-pool of mRNAs contained locally and ready to be translated within minutes of some neural activity, and a translocalized pool that may be delivered to distal sites within the dendrite approximately 30 minutes after activity. The timing of the local

protein synthesis requirement in studies of synaptic plasticity was generally within minutes of the stimulation protocol, arguing that at least the ready pool is required for synaptic plasticity to occur. Activity dependent translocation of mRNAs may serve to replenish members of the ready pool or as an additional level of spatio-temporal regulation of local protein synthesis. More research must be done to determine what mRNAs belong to which of these two pools and to determine what functional significance, if any, accessing mRNA from one pool over another serves.

1.3 Gene Expression Profiling and Memory

As the role of protein synthesis in memory was becoming more fully appreciated, speculation grew regarding what classes of proteins might be necessary. In keeping with the view that it is changes in the strength of neuronal interactions that ultimately result in the formation of memory, Barondes and Squire hypothesized that the required set of proteins would be “1) enzymes which regulate the synthesis or destruction of neurotransmitters; 2) receptor molecules in the post-synaptic neuron; 3) structural proteins; or 4) proteins which direct specialized types of intercellular recognition.”[45]

The rise of molecular biological techniques allowed researchers to finally begin identifying and studying these proteins. Because translation of a protein was thought to be correlated with the abundance of its mRNA, many early genetic studies of memory focused on transcriptional changes occurring after learning. A class of genes whose abundance was growth factor stimulated was first identified in non-neuronal cells[46].

Such so-called immediate early genes (IEGs) were subsequently found to also be induced

in neuronal cells following neurotransmitter mediated stimulation[47,48]. The expression of IEGs goes up during the hours following neuronal activity and represent a diverse array of functions [49]. Many of these genes coded for transcriptional regulators [50] and thus represented a fifth class of proteins that might be responsible for sustaining long term memory. This class of proteins it is reasoned, play a role in stabilizing the memory by altering the expression of downstream effector genes.

Using *in situ* hybridization assays, it is possible to visualize the expression of IEGs after neuronal activity. *Arc*, a cytoskeletal protein found to coprecipitate with F-Actin, had low basal mRNA levels within the hippocampus. However, after induction of synaptic activity, *Arc* mRNA expression rapidly increased and was found to localize within both somata and dendrites [51,52] and disrupting *Arc* expression led to deficits in synaptic plasticity and memory[53]. Later work showed that *Arc* was further localized within recently activated portions of dendritic shafts and synapses [24].

1.3.1 Next generation tools for studying protein synthesis in memory

The early progress made thanks to classic molecular biological techniques, while substantial, was limited in two respects: 1) these approaches were low-throughput allowing the researcher to study only a handful of genes at a time, and 2) they were candidate-based and so couldn't provide an unbiased view of potential translational changes that might be involved in memory. Advances in genetics would eventually eliminate both of these issues in future studies. The rise of gene-chip experiments, better known as microarrays, allowed the first high-throughput screens of gene expression

changes occurring during memory. A microarray contains hundreds or thousands of cDNA probes which hybridize to DNA or RNA isolated from biological samples. The probes are tagged and, upon hybridization and excitement with a laser, they fluoresce. The level of fluorescence is correlated with the abundance of the mRNA for that probe in the sample [54]. In one study, microarrays were used to study transcriptional changes that occurred in the hippocampus of rats following a spatial learning task. Rats were trained on the Morris water maze task in which they were required to learn the location of a platform in a pool of water. RNA was isolated from the hippocampus of trained and untrained rats at timepoints from 1 hour to 24 hours after training and was subsequently measured by microarray. Memory related genes were identified, the functions of which aligned strikingly well with those that Barondes and Squire had originally hypothesized [55]. Many other studies have successfully used microarray technology to identify memory related genes [56–60] but these studies were limited to pre-defined probe sets which had to be selected prior to the microarray. Because of this, novel gene isoforms could not be detected. In addition, because microarrays contain a set number of cDNA probes, there is an upper limit to the amount of DNA or RNA they can detect. A new technology that could measure gene expression for the entire genome in an unbiased way and which had no upper threshold for detection was needed to capture the full extent of gene expression changes occurring during memory.

The invention of RNAseq solved these issues. Unlike hybridization based approaches sequencing approaches directly identify the sequence of cDNA fragments in a sample. Traditional sequencing methods which analyzed single transcripts individually

were too low throughput and far too expensive to be done routinely on a genome wide scale. RNAseq solved this issue, allowing for massively parallel analysis of many RNA fragments at a time. Briefly, cDNA libraries are made from RNA fragments collected from biological samples and indexed adapters are ligated to both ends of the fragments. These cDNA molecules are then sequenced from one or both ends creating individual “reads” which are aligned to a reference genome and subjected to a variety of downstream analyses [61]. The emergence of this technology allowed for unbiased screens of gene expression, including analysis of splicing variants within a sample [62].

A major consideration for gene expression studies is how mRNA is collected and processed for RNAseq. Although there is some evidence that local translation of proteins in non-neuronal cells may play a role in synaptic regulation affecting learning and memory [63], the vast majority of studies have focused on the well documented requirement for protein synthesis in neurons. Thus it is important to determine that the mRNA being collected and analyzed using RNAseq is coming from the correct cell-type. Furthermore, it has become clear that despite initial impressions to the contrary, mRNA abundance has poor correlation with protein abundance [64–67]. To account for this, several methods of mRNA collection have been utilized. I will briefly summarize them below.

Early methods for collection of mRNA enriched for or exclusively containing single cell-types included laser capture microdissection (LCM) and fluorescence activated cell-sorting (FACS). LCM, first developed by Michael Emmert-Buck et al. in

1996 [68], allows visualization and isolation of a specific cell or cells. However, the technique requires fixation of the tissue which can degrade RNA molecules and is prone to contamination from neighboring cell-types [69]. FACS on the other hand can be done on fresh tissue and, thanks to the addition of a fluorescent marker for the cell-type of interest, either added during collection by immunostaining or encoded genetically, the likelihood of including cell-types other than the one of interest is relatively minor. One limitation of cell-sorting methods is that they require enzymatic dissociation of the isolated brain tissue and there is some evidence that the dissociation process can, itself, alter the gene expression profile [70].

These methods for isolating RNA from specific cell-types can be combined with a variety of biochemical techniques that allow researchers to address specific questions. As mentioned above, the abundance of an mRNA was found to be poorly correlated with the abundance of the protein for said gene. There are currently three common approaches to address this problem, all of which are based on the well documented idea that the rate limiting step in translation of an individual mRNA is initiation, during which the complete ribosomal complex is loaded onto the mRNA [71]. The classic approach, called polysome profiling, uses a sucrose gradient and centrifugation to separate mRNAs that are bound to one or more ribosomes from mRNAs that are unbound and so unlikely to be actively translating. Two more recent approaches have since been developed. The first is a technique known as ribosome footprint profiling [72]. In this technique, ribosome bound mRNAs are enzymatically digested, leaving only the ribosome-protected portion of the mRNA molecule available for deep sequencing. This allows for highly sensitive

detection of ribosome placement along an mRNA and is useful for determining translational efficiency of an mRNA, however regulatory features within the untranslated regions of the mRNA are destroyed in the process limiting what analyses can be done in these experiments. The final approach is translating ribosome affinity purification [73] or TRAP. Because TRAP is the preferred method of translational profiling used in our lab I will describe it in slightly greater detail below.

TRAP uses a genetically encoded enhanced Green Fluorescent Protein-tagged version of the ribosomal subunit L10a (EGFP-L10a) to allow immunopurification of ribosomes containing this subunit. The addition of the elongation blocking chemical cyclohexamide prevents mRNA from being redistributed into the non-ribosome bound pool during the collection process. Our lab has successfully used this technique to isolate mRNA from specific cell-types in the brain [74–76]. As with polysome profiling, and in contrast to ribosome footprint profiling, there is no digestion step which allows analysis of untranslated regions that may contain important regulatory information. TRAP has the additional advantage over these other methods of mRNA collection of being directly cell-type specific. Freshly dissected tissue may be homogenized and immediately processed, eliminating the need for fixation, enzymatic dissociation or lengthy cell sorting techniques. However, although the majority of translational regulation occurs at the initiation step, ribosomes have been shown to stall during elongation [77]. Thus, an important caveat for TRAP studies is that ribosome-bound mRNA may not be actively translating.

1.3.2 Recent translational profiling studies of protein synthesis during memory

The development of these translational profiling tools has led to a slew of new research aimed at taking an unbiased approach to discovering which proteins are synthesized during synaptic plasticity and memory and what signaling pathways ultimately control this process. The first unbiased next-generation study to predict mRNAs localized to dendrites was performed by Ivan Cajigas et al in 2012 [78]. In this study they micro-dissected neuropil from stratum radiatum and isolated mRNAs from this tissue. Because their study did not utilize a cell-type specific method for isolating mRNA, they filtered from their lists any genes that were thought to be restricted to non-neuronal cell-types or to the nucleus. Their final list contained 2,550 genes thought to be localized to dendrites suggesting a previously unappreciated diversity of potentially locally synthesized proteins. In 2014, Joshua Ainsley from our own lab published a study utilizing the TRAP method of mRNA isolation proposing 1,890 mRNAs which mostly did not overlap with the Cajigas list [74]. In this study more than 800 genes which had been filtered from the Cajigas list were shown to be dendritically localized, including several which had previously been thought to be restricted to the nucleus but which were confirmed to be dendritically localized by *in situ* hybridizations.

Other studies have effectively used these next generation tools to push forward our understanding of translational changes that occur in the minutes and hours following neuronal activation. In 2015, Jun Cho et al [79] used ribosome footprint profiling to detect alterations in translation efficiency in the hippocampus at 5 minutes, 10 minutes, 30 minutes and 4 hours following contextual fear conditioning. They found that

translational repression, rather than translational upregulation were major features of this time course and that this repression was mediated at least in part by inhibition of the Estrogen receptor 1 (ESR1) pathway. In contrast, a study by Patrick Chen et al. in 2017 [80] showed that the of majority differentially expressed (DE) genes were upregulated during the short time course after synaptic plasticity in hippocampal slice, although downregulation was seen at later time-points. Chen et al. also found that TRAP improved their detection of differentially expressed genes over total RNA-seq.

1.4 Contributions of this Thesis

It is into this body of work that we submit our findings. In this thesis I will present what is, to my knowledge, the first *in vivo* translational profiling study of the time course of local protein synthesis within CA1 hippocampal dendrites following contextual fear learning. This work is presented in two parts. In part one I will present a follow-up to the study in Ainsley et al. [74] in which we add to the list of dendritically predicted mRNAs and compare features of mRNAs that are preferentially enriched in dendrites or somata. These data were generated from 30 individual mice and represent a substantial expansion of mouse numbers used in the previous study. We find 2,923 genes predicted to be in dendrites, the largest list of dendritically predicted mRNAs to date. Our list adds supporting evidence for many previously identified dendritic mRNA candidates and identifies a new set of candidate mRNAs.

In part two, we analyze the time-course over which our ribosome-bound dendritic mRNAs were collected and present our findings on the temporal dynamics of ribosome-

mRNA binding. Our findings clarify outstanding questions regarding the preference for repression or enhancement of translation during the early time points following neuronal activation. We find that early upregulation in ribosome binding immediately following contextual fear conditioning in dendrites is followed by repression of ribosome binding at 15 minutes following fear conditioning.

It is our hope that the data presented here will add to our understanding of local protein synthesis as it relates to the formation of long term memory. We further hope that the supplementary tables which include our list of predicted dendritically localized genes will serve as a resource to the field at large.

Chapter 2: Methodology

2.1 Animals

All animal procedures were performed in accordance with the National Institutes of Health Guide for the Care and Use of Laboratory Animals and were approved by the Tufts University Institutional Animal Care and Use Committee. Mice used for this study were heterozygous for two transgenes: tetracycline transactivator protein (tTA) under control of the *Camk2a* promoter, and EGFP-L10a fusion protein under the tetracycline operon (tetO). Mice had access to food and water ad libitum and were socially housed with littermates prior to the start of any experiment. Mice were kept on a normal light-dark cycle of 14h light/10h dark. All experiments were performed during the light phase. For transferring mice during experiments, mice were handled by the tail. Mice were generally between 10-12 weeks of age at the start of each experiment.

2.2 Fear Conditioning

At least 3 days prior to the start of any behavioral experiment, mice were placed in single housing to minimize the amount of hippocampal activation occurring during the resting state. Cages were not disturbed following single housing until the day of the experiment. On the day of the experiment, mice were transported from our animal housing room to a separate room which houses our fear conditioning apparatus. Mice were transported in their home cages placed inside an opaque paper bag to minimize visual stimulus prior to the onset of fear conditioning. At the beginning of the experimental day, and between fear conditioning sessions, all surfaces, grids and trays inside the apparatus were cleaned. All urine and feces were removed and surfaces were

wiped down with 70% ethanol to remove odors from previous animals that had been placed in the conditioning boxes and to provide a consistent contextual cue.

All fear conditioning was performed during the same time of day between 09:00:00 am and 10:30:00 am. Mice were received one contextual fear conditioning trial. Fear conditioning trials lasted 500 seconds and were performed using the Coulbourn Instruments; H10-11RTC, 120W x 100D x 120H. Each 500 second trial consisted of 4, 2 second long, 0.7 mA foot shocks administered at 198, 278, 358, and 438 seconds. Mice were sacrificed immediately, 15 minutes or 30 minutes following fear conditioning. If mice were not sacrificed immediately they were returned to their home cages and transported back to the animal housing room prior to sacrificing them.

2.3 mRNA Isolation and Immunoprecipitation

All RNA handling was performed at lab benches that had been thoroughly cleaned with bleach, 70% ethanol, and RNase Zap (Invitrogen) to remove contaminating DNA and RNA degrading enzymes. RNA isolation was performed using a modified version of the detailed Translating Ribosome Affinity Purification (TRAP) technique published by Heiman et al. [73,81,82] that was optimized to remove background [74]. An anti-GFP antibody (HtzGFP-19C8) from the Monoclonal Antibody Core Facility at the Memorial Sloan-Kettering Cancer Center was covalently bound to magnetic epoxy beads (Invitrogen) followed by BSA treatment to reduce non-specific binding. Following behavioral testing, mice were anesthetized using isoflurane. Mice were decapitated and the head was submerged in ice-cold dissection buffer (1x HBSS, 2.5 mM HEPES-KOH,

35 mM glucose, 4 mM NaHCO₃). The brain was removed, rinsed briefly in fresh dissection buffer and placed into an ice cold brain slicer matrix (Zivic Instruments). Between 2 and 4 coronal slices were made through the anterior portion of the hippocampus, each 0.5mm thick. Slices were placed on a cold petri-dish that had been filled with ice. Homogenization buffer [82] containing cycloheximide was added to each slice in order to pause translocation of ribosomes. Brain slices were micro-dissected to isolate CA1 stratum pyramidale and stratum radiatum tissue sections. Cortical and striatal tissue was peeled away from the hippocampus. A cut just lateral to CA1 was made to remove CA3. Another cut was made along the ventral side to remove dentate gyrus. Finally, stratum pyramidale was separated from stratum radiatum with a single cut along the border between the two regions (Figure 3.1). Each micro-dissection was added to 150µl of homogenization buffer and homogenized using an automatic pestle.

Homogenized samples were centrifuged at 2,000 x g for 10 minutes, lysate was moved to a clean tube and centrifuged at 20,000 x g for 15 minutes. All centrifugations were done at 4°C. The lysate was transferred to a clean tube containing the Anti-GFP-L10a coated beads. Samples were incubated with the beads for 1 hour at 4°C with end-over-end rotation. The supernatant (SN) was saved for comparison to the immunopurified samples (IP). After five washes with 0.5ml of KCl buffer, RNA was extracted with Trizol LS. The back extraction described in Ainsley et al [74] was omitted because it was found not to improve yield in our study. RNA was precipitated using NaOAc, isopropanol, and linear acrylamide overnight at -80°C. After two washes with 80% EtOH, the RNA was resuspended in 12 µl nuclease-free water.

2.4 Quantitative RT-PCR and Bioanalyzer Analysis

In order to remove genomic DNA contamination, mRNA samples were treated for 30 minutes with TURBO DNase (Ambion) prior to any downstream applications. RNA was re-isolated with Trizol LS as described above to remove DNase. RNA yield and quality measurements were taken using the Agilent Technologies 2100 Bioanalyzer using RNA Pico chips and according to the manufacturer's instructions. cDNA libraries were prepared using reverse transcription (RT) with Superscript III (Invitrogen) using a combination of random hexamers and anchored-oligo dT primers in order to minimize 3' UTR bias associated with reverse transcription by anchored-oligo dT alone. Quantitative RT-PCR was performed with SYBR Green PCR master mix (Applied Biosystems) on either the Mx3000P thermo cycler (Agilent) or the StepOne thermo cycler (Applied Biosystems). Primers used are listed in table 2.1 below. Deenrichment of non-neuronal genes in the IP was determined by the $\Delta\Delta\text{ct}$ method ($\Delta\Delta\text{ct} = \Delta\text{ct}_1 - \Delta\text{ct}_2$). Δct_1 was calculated as the expression of *Gfap* (negative control, expressed in astrocytes) in the IP normalized for the expression of *Gfap* in the IP ($\Delta\text{ct}_1 = Gfap \text{ IP ct} - Gfap \text{ SN ct}$), and Δct_2 represented the normalized expression of *Camk2a* (positive control, expressed in CA1 projection neurons) in the IP ($\Delta\text{ct}_2 = Camk2a \text{ IP ct} - Camk2a \text{ SN ct}$). Larger $\Delta\Delta\text{ct}$ values indicated greater de-enrichment of non-neuronal genes and therefore a more successful IP. Correct placement of the micro-dissection was determined by *Wfs1* which is only expressed in cell bodies of CA1 projection neurons. *Wfs1* Δct was calculated ($Wfs1 \Delta\text{ct} = Wfs1 \text{ ct} - Camk2a \text{ ct}$) for dendrite and soma samples. Micro-dissections were considered correctly placed if *Wfs1* Δct was at least 2X larger in the dendrite or if *Wfs1*

was undetectable in the dendrite.

Table 2.1. qPCR primer sequences.

Gene name	Primer sequence
Gfap_F	5'-CGGAGACGCATCACCTCTG-3'
Gfap_R	5'-AGGGAGTGGAGGAGTCATTCG-3'
Camk2a_F	5'-TTTGAGGAACTGGGAAAGGG-3'
Camk2a_R	5'-CATGGAGTCGGACGATATTGG-3'
Wfs1_F	5'-GGATGAAGATGAGGACGAGC-3'
Wfs1_R	5'-TGATGGGTGGGTACAATGGT-3'

2.5 Library preparation and RNA-sequencing

Because RNA concentration was low, RNA samples were amplified and converted to complementary DNA using the Ovation RNA-Seq V2 Kit (Nugen) according to the manufacturer's instructions. This kit is optimized to reduce RNA sequences contained in ribosomal RNA and uses a combination of oligo dT and random primers in order to reduce 3' end bias. Libraries were prepared and barcoded using the TruSeq Nano DNA Kit (Illumina), according to the manufacturer's instructions. Barcoded libraries were multiplexed and sequenced on the HiSeq2500 at the Tufts University Core Facility. Libraries were sequenced using the high output mode for 50 bp single end sequencing.

Sequencing quality control was performed using FastQC (Barbraham Institute). Reads were aligned using STAR (version 2.3.0e)[83] Unique read counts per gene were determined using HTSeq (version 0.6.1p) [84] and used for intersample comparisons and differential expression analysis. Clustering analysis was performed on count data using variance stabilizing transformation as part of the DESeq2 R package [85]. Differential expression analysis was also carried out using DESeq2. For all differential expression analyses, a term to model a sequencing batch effect found in our data was included in the design in addition to the term for our comparison of interest. When the differential expression analysis was performed by negative binomial likelihood ratio test the batch effect was used as the reduced model. Cufflinks (version 2.0.2) was used to generate FPKM (fragments per kilobase of transcript per million mapped reads) with ribosomal and mitochondrial sequences masked. Gene annotations and genome files were obtained from Gencode [86] (Release version GRCm38, Gencode version M17). GO analysis was performed using DAVID (<https://david.ncifcrf.gov>) [87,88] Dendritic prediction scores were calculated using a logistic regression algorithm in R.

2.6 Tissue preparation and immunohistochemistry

A small group of mice were used for immunohistochemistry to check expression of the EGFP-L10a fusion protein. Mice were deeply anesthetized with ketamine/xylazine and perfused transcardially with ice cold 0.1M phosphate buffer for 1 min at a rate of 15 ml/min followed by ice-cold 4% paraformaldehyde (PFA) in 0.1M phosphate buffer for 5

min at a rate of 15 ml/min. Brains were removed and post-fixed in 4% PFA overnight at 4°C. Brains were transferred to 30% sucrose for 48-72 hours at 4°C, and then snap-frozen in -50°C isopentane for 3 min. Frozen brains were stored wrapped in parafilm in air-tight containers at -20°C until sectioning. Coronal brain sections were sliced at 20µm using a cryostat and immediately placed in 1X PBS at room temperature. Sections were stored at -20°C in a glycerol-based cryoprotectant and protected from light until use.

For immunohistochemistry, free-floating brain sections were washed in a solution of 1X PBS overnight at 4°C to remove any excess cryoprotectant. All washes were done with gentle agitation while protected from light. Sections were rinsed three times for 15 minutes in 1X PBS with 0.25% Triton-X-100 (PBS-T). Sections were then blocked at room temperature for 1 hour in PBS-T containing 10% normal goat serum. Primary antibody for GFP (Aves chicken anti-GFP, polyclonal, 1:500) was diluted in blocking solution and incubated overnight at 4°C with gentle agitation, while protected from light. Sections were washed three times for 20 min in PBS-T. Secondary antibody (Jackson Immuno research, goat anti-chicken DyLight 488 1:500) was diluted in blocking solution and applied to the sections for 2 hours at room temperature. Sections were washed three times for 15 min in 1X PBS. Sections were mounted onto slides, coverslipped using Prolong Gold Anti-fade Mounting Media, stored at 4°C and protected from light until imaging.

2.7 Microscopy

To detect EGFP-L10a expression, images were acquired using a Nikon A1R

confocal laser scanning microscope using 20X air or 60X oil objectives. We used 488 nm excitation lines and band-pass emission filters of 500-550 nm (GFP) were used.. 1024 x 1024 resolution images were acquired using an average of 2 line scans with a 1.1 pixel dwell time. Z sections with 1 μ m step size were taken.

2.8 Statistical analysis

All statistical analysis was done in the R statistical programming language. Error bars represent +/- SEM. Comparisons between groups were found using one-tailed Welch's t-tests for normally distributed variables and values are considered statistically significant with $p < 0.05$. For differential expression analysis, multiple comparison corrections were done using the Benjamini Hochberg algorithm [89] and values were considered statistically significant if the adjusted p-value, $p_{adj} < 0.1$.

Chapter 3: Results

3.1 Diverse pools of mRNAs localize to discrete neuronal compartments

A previous study in our lab used the TRAP methodology to define the set of ribosome-bound mRNAs that are present in dendrites [74]. Although TRAP has clear advantages over other methods of mRNA isolation which have been used to study dendritically localized mRNAs [78,90] (described above), this study was limited in two respects. 1) Translational profiling of dendrite and soma samples was carried out only on mice that had not undergone any behavioral training paradigm or on mice that had been sacrificed immediately after fear conditioning. This approach is likely to miss many important changes in translation that occur in the minutes following learning. 2) Predictions for dendritically localized mRNAs were ultimately based on very low numbers of mice. Therefore, in order to determine the complete list of dendritically localized mRNAs it was important that we addressed these limitations in the current study.

3.1.1 Isolation of mRNA from CA1 projection neuron dendrites and somata.

In order to isolate mRNA from dendrites and somata within CA1 projection neurons, we used a mouse line that had been previously generated in our lab [75]. Enhanced green fluorescent protein-tagged ribosomal subunit L10a (EGFP-L10a) is expressed via the tetracycline transactivator (tTA-TetO) system under the control of the Camk2a promoter [91]. EGFP-L10a is strongly expressed in projection neurons that reside in the CA1 of the hippocampus in this mouse (Figure 3.1A). The hippocampus is a highly laminar structure. Expression of EGFP was detectable in both somata of these

neurons which reside in the stratum pyramidale of the hippocampus as well as within dendritic branches which extend into the stratum radiatum. We therefore separately collected hippocampal tissue from the stratum pyramidale and stratum radiatum and categorized these as soma samples and dendrite samples respectively . In contrast to our previous study which collected tissue punches from flash frozen hippocampal slices, micro-dissections were performed fresh in order to minimize freeze-fracture of the mRNA molecules in our samples (Figure 3.1B). During learning, neuronal activity drives changes in translation within both dendrites and somata. We were interested in measuring changes in the translational profiles during the early time course following a hippocampal learning paradigm that was likely to be due to specific alterations in ribosome binding rather than broad changes in mRNA expression due mostly to *de novo* transcription. We therefore considered a narrow timeframe for mRNA collection from CA1 dendrites and somata that would meet this criteria. In a study from 1999, Guzowski et al tracked the time it took for *Arc* mRNA to move from the nucleus to the cytoplasm in the hippocampus after interaction with a novel environment. They found that *Arc* cleared the nucleus and had entered the cytoplasm within 30 minutes [92]. We therefore collected mRNA from CA1 dendrites and somata at several points during the first 30 minutes after a hippocampal learning task. Because previous studies have suggested that ribosomal granules may travel into the dendritic shaft from somata within 30 minutes of neuronal activity [42,43], this time course allows us to capture the early changes in ribosome binding occurring within dendrites potentially including those due to translocalization from somata. Specifically, prior to micro-dissection, mice were fear conditioned

following a contextual fear conditioning protocol (Figure 3.1C and see methods) and either sacrificed immediately (FC0) or allowed to recover in their home cage for fifteen or thirty minutes prior to sacrifice (FC15 and FC30 respectively). A subset of mice were taken directly from their home cages and sacrificed (HC). Upon sacrifice, all mice immediately had their brain removed, slices from the hippocampal region prepared and micro-dissections performed in the presence of cycloheximide to prevent ribosome dissociation from the mRNAs. mRNA from *Camk2a*-expressing neurons was then isolated from dendrite and soma samples by TRAP immunopurification. Both the neuron enriched, ribosome-bound mRNA (IP; immunopurified) samples and flow-through mRNA (SN; supernatant) samples were collected.

The quality, sizing and concentration of mRNA samples was measured by Agilent Bioanalyzer (Figure 3.1D). The quality of the mRNA was determined by RIN score which takes into account the shape of the entire RNA electropherogram trace to determine levels of RNA degradation [93]. Dendrite IP samples had an average RIN of 6.5 and Soma IP samples had an average RIN of 7.5. SN samples had poorer RIN values (dendrite SN average = 5.3; soma SN average = 5.5). The difference in RIN value was likely due to a depletion of 28s ribosomal RNA in SN samples (Figure 3.1D). This phenomenon is consistent with the idea that free-floating 60s ribosomal subunits will be slightly depleted in SN samples during the TRAP protocol. Also consistent with a successful TRAP immunopurification is the depletion of small RNAs seen in IP but not SN samples (Figure 3.1D) which may also contribute to lower RIN scores in SN samples.

As we have seen previously, RNA concentrations for IP samples are in the hundreds of picograms range[74].

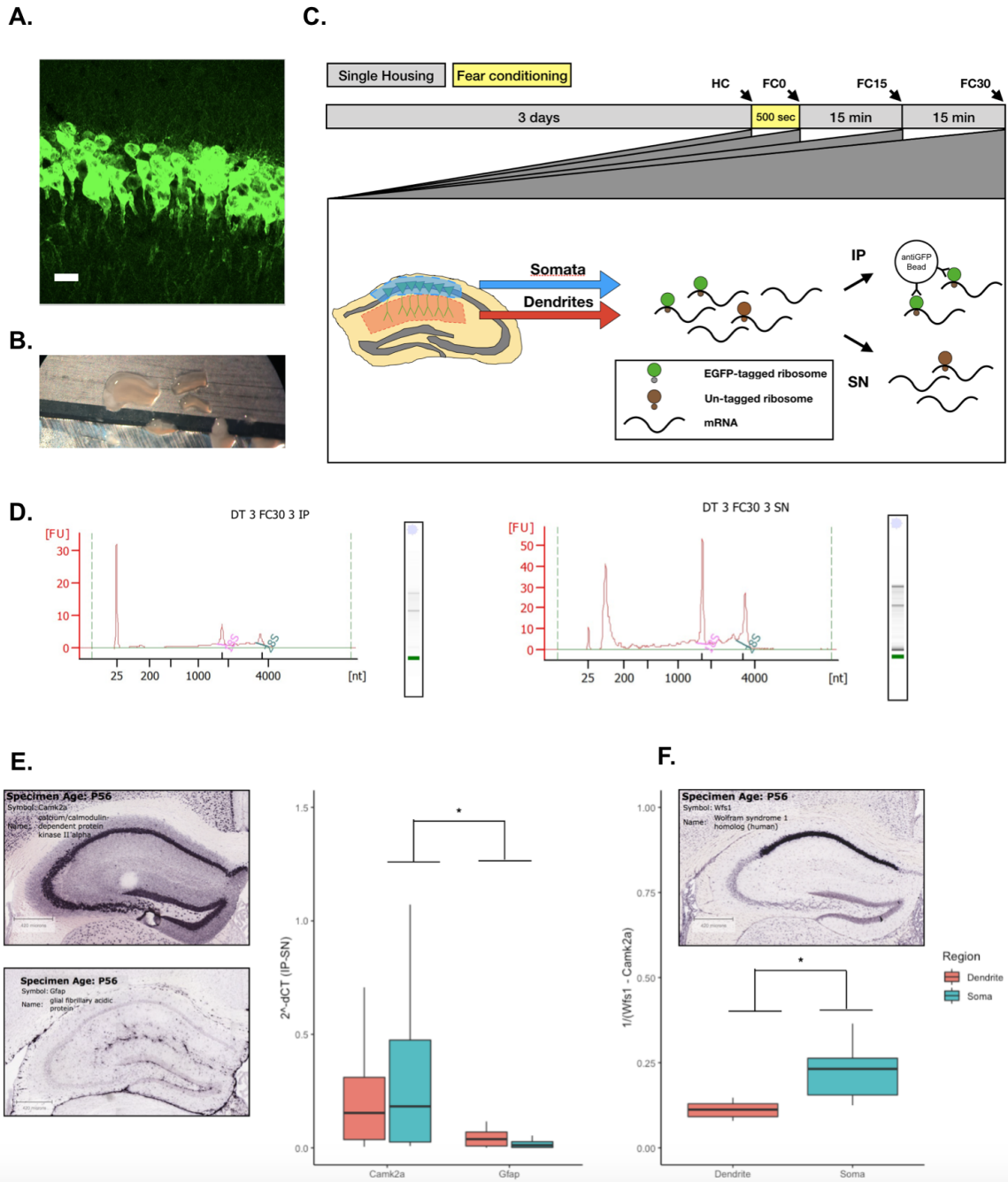


Figure 3.1 Collection of dendritic and somatic mRNA by TRAP. A) EGFP-L10a expression in the dorsal CA1 of a Camk2a-EGFP-L10a mouse. EGFP-L10a is detected in both the somata and the dendrites of CA1 projection neurons. Scale bar = 20 um. B) Micro-dissection of a 0.5 mm thick bilateral hippocampal section. Left hippocampus has not yet been micro-dissected. Right hippocampus has had dentate gyrus removed and has been separated into stratum pyramidale (top) and stratum radiatum (bottom) sections. C) Experimental design for mRNA collection. Mice were singly housed for three days and subjected to one 500 second fear conditioning session. Mice micro-dissected at 0 minutes, 15 minutes or 30 minutes after fear conditioning and subjected to TRAP immunopurification. IP samples containing mRNAs bound to EGFP-tagged ribosomes from Camk2a expressing neurons and SN samples containing a mixture of mRNAs bound to un-tagged ribosomes and unbound mRNAs were collected. D) Representative bioanalyzer traces from IP and SN samples. IP samples are depleted for small RNAs in the 25-200 bp range. E) qPCR results for a positive (Camk2a) and negative (Gfap) control genes. IP samples are relatively de-enriched for Gfap versus Camk2a compared with their respective SN samples. For visual clarity, data are presented as $2^{-(Ct(IP) - Ct(SN))}$. P-value < 0.05. F) qPCR results for CA1 projection neuron cell body marker Wfs1. Dendrite samples are relatively de-enriched for Wfs1 versus Camk2a compared to Soma samples. For visual clarity, data are presented as $1/(Ct(Wfs1) - Ct(Camk2a))$. P-value < 0.05.

Successful depletion of non-neuronal mRNAs from the IP samples during the TRAP protocol was measured by qPCR. Primers for *Camk2a* and the glial gene *Gfap* were used as positive and negative controls respectively. Dendrite and soma IP samples were enriched for Camk2a compared with SN samples (Figure 3.1E). We confirmed placement of the microdissection by testing for the presence of gene *Wfs1*. *Wfs1* is present at high levels within CA1 projection neuron cell bodies, but, unlike *Camk2a* which is expressed in both the stratum pyramidale and stratum radiatum of the CA1 (Figure 3.1E and [38,39]), *Wfs1* is not expressed within the stratum radiatum (Figure 3.1F). Dendrite samples were de-enriched for *Wfs1* mRNA as compared with soma samples by qPCR.

3.1.2 Translational profiling of discrete subcellular compartments of CA1 Projection neurons

We used RNA sequencing (RNA-seq) to determine the genome-wide gene expression patterns within dendrites and somata. Samples were classified as one of: dendrite IP (mRNAs bound to EGFP-L10a tagged ribosomes originating from stratum radiatum dissections), soma IP (mRNAs bound to EGFP-L10a tagged ribosomes originating from stratum pyramidale dissections), dendrite SN (mRNAs not bound to tagged ribosomes originating from stratum radiatum dissections) and soma SN (mRNAs not bound to tagged ribosomes originating from stratum pyramidale dissections). Dendrite SN and soma SN samples include mRNAs not bound to ribosomes originating in CA1 pyramidal neurons as well as a mixture of mRNAs originating from other cell types that were located within the dissected region (Figure 3.1C) and thus are treated as a measure of background mRNA expression in those regions. RNA-seq reads were aligned to the mouse genome. Uniquely mapped reads accounted for greater than 75% of reads in all samples (Supplementary Table 1; all supplementary tables are available on proquest). Aligned reads were then used to calculate counts for every gene. Given the differences in biological point of origin for each sample type we hypothesized that genome-wide expression profiles for these samples would segregate based primarily along two vectors: 1) whether they were ribosome-bound (portion; IP/SN) and 2) where the micro-dissection was placed (region; dendrite/soma). To test this we performed principal component analysis (PCA) of the gene-count data for all samples (Figure 3.2A). Further analysis revealed that the samples also segregated in a way that was not reflected in the

underlying biology along the first principal component. This non-biological effect correlated very well with which of two batches of sequencing the sample had been included in (Figure 3.2B and Supplementary Table 1). Downstream analyses were thus careful to account for the presence of this batch effect (see methods).

Having access to genome-wide RNA-seq data, we wanted to further confirm the success of our TRAP immunopurification. We used available single-cell datasets [94] to generate a list of control genes. Positive control genes were selected such that they are expressed in CA1 pyramidal neurons but not other cell types present in the CA1 region, while negative control genes are not expressed in CA1 pyramidal neurons. Expression patterns for these genes were validated using the Allen Brain Institute *in situ* hybridization atlas (Supplementary Table 2). We tested for fold-change differences between the IP and SN portions for dendrite and soma samples (Figure 3.2C-D). Differential expression testing was performed using DESeq2 [89] which uses generalized linear models to estimate fold changes. Based on this analysis there were 7,802 genes differentially expressed between IP and SN in the dendrite samples (4,529 genes enriched in IP with \log_2 fold changes > 0 ; 3,273 genes enriched in SN with \log_2 fold changes < 0 ; false-discovery rate of < 0.1) and 6,620 genes differentially expressed between IP and SN in the soma samples (3,094 genes enriched in IP [i.e. \log_2 fold changes > 0]; 3,526 genes enriched in SN [i.e. \log_2 fold changes < 0]; adjusted p-value < 0.1). As expected, we found that positive control genes were enriched in IP samples while negative control genes were enriched in SN samples in both dendrites and somata (Figure 3.2C-D).

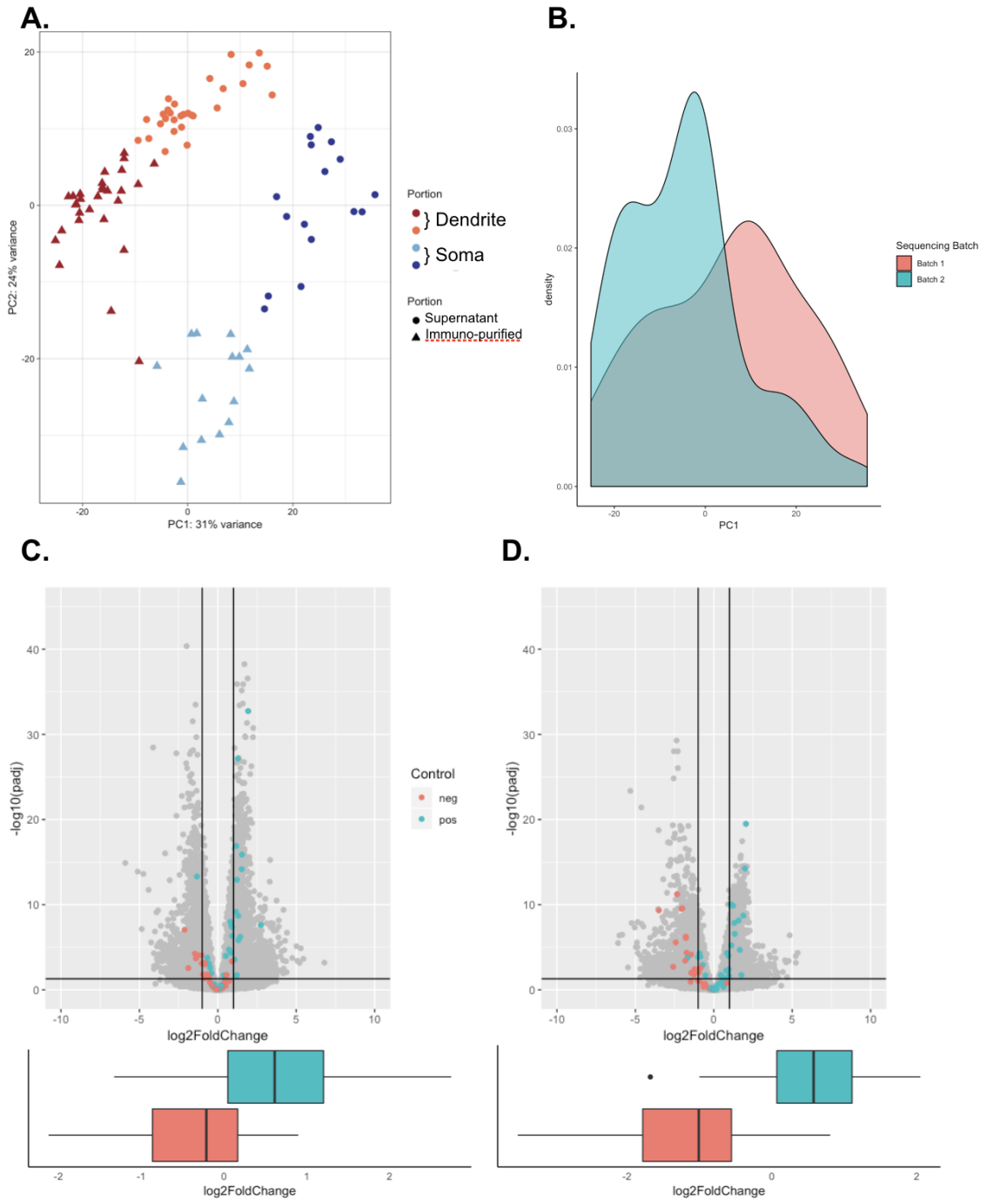


Figure 3.2 RNA-seq confirms specificity of TRAP mRNA collection. A) Principal component analysis of normalized gene counts for all samples. The first two principal components (accounting for 31% and 24% of the variance respectively) separate samples based on which region their micro-dissection was collected from, and whether the sample was in the IP or the SN portion. B) Density plot of the first principal component with samples grouped by two separate batches of RNA-sequencing. Samples separate along PC1 indicating the presence of a batch effect for these samples. C) Top: Volcano plots of differential expression of genes in dendrite IP vs dendrite SN samples. Positive (“pos”) and negative (“neg”) control genes are shown. Vertical lines are plotted at +/- 2-fold enrichment. Horizontal line is plotted at adjusted p-value (padj) < 0.1. Bottom: Boxplots showing the log2-fold change for positive and negative control genes. Positive fold-change represents enrichment in the IP, negative fold-change represents enrichment in the SN. Positive control genes are more enriched in dendrite IP and negative control genes are more enriched in dendrite SN. D) As in C but for Soma IP vs Soma SN samples. Positive control genes are more enriched in soma IP and negative control genes are more enriched in soma SN.

Given the functional differences between these two cellular compartments, we hypothesized that different mRNA pools are present within dendrites and somata. We therefore calculated estimated fold changes between dendrite-IP and soma-IP samples (Figure 3.3A). We found 4,756 genes to be differentially expressed between these samples. Given that individual dendrites contain relatively few mRNAs compared with their somata [95], it was striking that nearly two-thirds of genes that were differentially expressed appeared to be enriched in dendrites (64% or 3,037 genes enriched in dendrite-IP [i.e. log₂ fold changes > 0] compared with 36% or 1,719 genes enriched in the soma [i.e. log₂ fold changes < 0]; adjusted p-value < 0.1). One possibility is that the IP samples contain contamination from mRNAs in the ribosome-unbound pool or from ribosome-bound mRNA in other cell-types. Indeed, the stratum radiatum from which the dendrite-

IP samples were collected is much more heterogeneous than the stratum pyramidale from which soma-IP samples were collected. Therefore we also calculated fold enrichment for dendrite-SN versus soma-SN samples. We found that 3,730 genes were differentially expressed between these two samples (Figure 3.3B). In contrast to IP samples, dendrite-SN and soma-SN enrichment were roughly even (53% or 2,005 genes enriched in dendrite-SN [i.e. \log_2 fold changes > 0] compared with 47% or 1,725 genes enriched in the soma [i.e. \log_2 fold changes < 0]; adjusted p-value < 0.1). It is possible that the relatively greater heterogeneity of cell-types within the stratum radiatum versus the stratum pyramidale gave rise to a more pronounced contamination that was exacerbated during PCR steps during RNA-seq library construction. If this were the case, genes that were enriched both in the IP and the SN of dendrites would contribute disproportionately compared with genes that were enriched both in the IP and the SN of somata. Figure 3.3C shows the overlap of enriched genes for each comparison. Filtering the differentially expressed gene lists from the IP to exclude genes that were also enriched in their respective SN had no effect on the percentages of genes that were enriched in either dendrite-IP or soma-IP (66% or 2,122 genes enriched in dendrite-IP versus 34% or 1,085 genes enriched in soma-IP; Figure 3.3D). These findings suggest that dendritic compartments have a greater diversity of mRNAs bound to ribosomes than does the somatic compartment within the early time-points after contextual fear conditioning measured in our study (22 out of 29 dendrite samples were obtained from fear-conditioned mice, with the remaining 7 samples obtained from home-cage mice; 11 out

of 15 soma samples were obtained from fear-conditioned mice, with the remaining 4 samples obtained from home-cage mice).

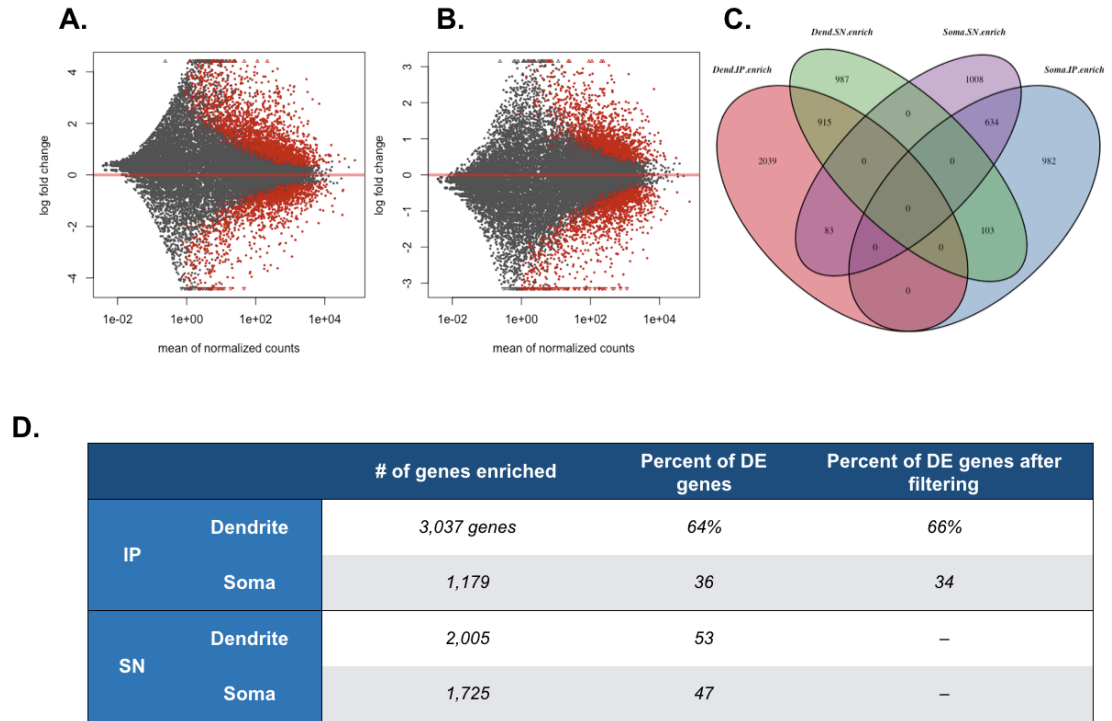


Figure 3.3 Differential expression analysis reveals greater diversity of ribosome-bound mRNAs in dendrites than somata. A) MA-plot of differential expression results between dendrite IP and soma IP samples. Positive log fold change indicates enrichment in the dendrite IP, negative log fold change indicates enrichment in the soma IP. Genes that were significantly differentially expressed (adjusted p-value < 0.1) are plotted in red. B) As in A but for dendrite SN and soma SN samples. C) Venn-diagram of overlapping enriched genes from comparisons in A and B. D) Table showing total numbers of enriched genes and percentage of all differentially expressed (DE) genes that were enriched in dendrite vs soma for IP and SN comparisons. For IP comparisons, genes that were enriched in SN comparisons were filtered out and the percentage of DE genes was recalculated. Nearly two-thirds of differentially expressed genes in IP comparisons were enriched in dendrites versus half of differentially expressed genes in SN comparisons enriched in dendrites.

3.1.3 Differences in regulatory elements of mRNAs enriched in dendrites or somata.

Much work has been done to parse the various means by which protein translation might be regulated. It has been shown for example that neuronal mRNAs contain on average much longer 3'UTR regions [96,97]. The 3'UTR is a potent site of translational regulation: 3'UTRs can contain targeting elements [38,39] in the sequence secondary structure which are required for correct localization of an mRNA as well as microRNA binding sites which target the mRNA for degradation and binding sites for RNA binding proteins which can regulate the level of translation [98]. Likewise, 5'UTR dependent mechanisms for regulation of translation are well studied, the most well understood of which are the 5'UTR cap-dependent mechanisms of translational regulation [5,6,9]. We were therefore interested in differences between these mRNA features in our RNA-seq data. SN samples collected from the cell layer of the stratum pyramidale are more enriched for neuronal cell bodies as compared with SN samples collected from the stratum radiatum which contain a mixture of background neuropil consisting of both neuronal and glial processes. Concurrently, mRNAs enriched in pyramidale contain, on average, much longer UTRs on both the 3' and 5' end, and this difference was more pronounced for 3'UTRs (Figure 3.4A; Pyramidale 5'UTR, 360.15 base pair average length, Radiatum 5'UTR 259.29 base pair average length, Welch Two Sample t-test p-value = 4.629e-14; Pyramidale 3'UTR, 2033.57 base pair average length, Radiatum 3'UTR 1055.03 base pair average length, Welch Two Sample t-test p-value = 2.2e-16). Strikingly, the reverse trend was apparent when comparing the ribosome bound IP samples. mRNAs enriched in dendrite IP samples contained, on average, longer UTRs on

both the 5' and 3' ends than mRNAs enriched in soma IP samples (Figure 3.4B; dendrite 5'UTR, 333.37 base pair average length, soma 5'UTR 290.667 base pair average length, Welch Two Sample t-test p-value = 0.0024; dendrite 3'UTR, 1569.38 base pair average length, soma 3'UTR 1354.937 base pair average length, Welch Two Sample t-test p-value = 1.59e-05). These data are consistent with the idea that local translation of dendritic mRNAs can preferentially use mRNAs with longer 3'UTRs [99].

The longer 5'UTR lengths observed in dendrites may be partially due to the inclusion of regulatory motifs contained within the sequence. One commonly used and well studied regulatory mechanism that is known to be involved in synaptic plasticity is the regulation of translational initiation mediated by mTORC1 [9,14]. mTORC1 specifically regulates the translation of a set of genes containing terminal oligopyrimidine (TOP) motifs. A large percentage of these genes encode proteins that are part of the translational machinery, including many ribosomal proteins. We have previously seen mRNAs which encode ribosomal proteins enriched in dendrites and were therefore curious if this phenomenon held true [74]. We measured how many mRNAs containing known TOP motifs were enriched in each comparison. Dendrite samples were enriched for TOP mRNAs in both the IP and SN portions compared with their respective soma portions (Figure 3.4C). Greater levels of dendrite enrichment compared with soma enrichment in SN samples may reflect a difference in the relative amounts of ribosome binding versus dendritic or somatic localization of these genes. Of the 16 TOP mRNAs enriched in dendrite IP samples, 3 encoded ribosomal proteins (*Rpl19*, *Rpl118*, *Rps15a*) confirming our previous findings.

RNA binding proteins can play a significant role in the localization and translational regulation of mRNAs. Fragile X mental retardation protein (FMRP) is known to play a role in localization and translational repression of mRNAs and loss of FMRP results in an impairment in structural plasticity – changes in spine morphology – that occurs after learning[100–103]. We therefore measured the total number of FMRP target genes enriched in each sample type, using the list of FMRP target genes generated by Darnell et al.[103] (Figure 3.4D). In the ribosome-bound IP portion dendrites were enriched for 2.5 times as many FMRP target mRNAs as somata, while in the SN portion, dendrite and soma layers were enriched for roughly equal numbers of FMRP target mRNAs. Dendritically enriched ribosome-bound FMRP target mRNAs had a high degree of overlap with dendrite SN enriched FMRP target mRNAs (72.3% of FMRP targets enriched in dendrite SN were also enriched in dendrite IP). This is higher than expected, as only ~30% of all dendrite IP genes overlap with dendrite SN genes (Figure 3.3C).

3.1.4 Prediction of dendritically localized mRNAs

Because our RNA-seq data indicate good separation of positive and negative control genes between IP and SN in dendrite samples (Figure 3.2) we used these data to generate a model to predict all potentially dendritic mRNAs. Although differential expression analysis can reveal genes enriched in the dendrite IP versus dendrite SN, this is an incomplete list of all possible dendritic mRNAs because it does not account for

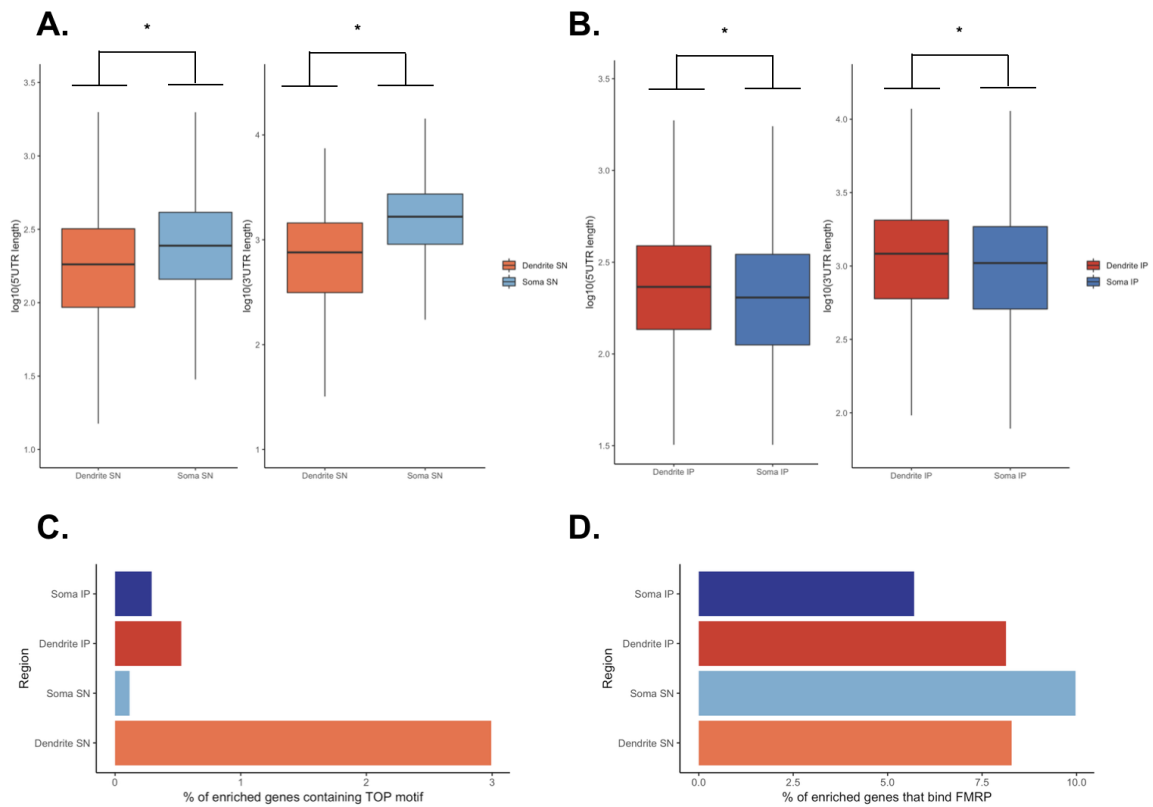


Figure 3.4 Ribosome-bound genes in dendrites and somata display alternate trends in UTR length and enrichment of certain regulatory features. A-B) Average 5'UTR and 3'UTR lengths for genes enriched in dendrite or soma. A) Genes enriched in soma SN have longer average 5'UTR and 3'UTR lengths than those that were enriched in dendrite SN. B) Genes enriched in dendrite IP have longer average 5'UTR and 3'UTR lengths than those that were enriched in soma IP. C) Percentage of genes enriched in dendrite or soma that contained known TOP motifs. D) Percentage of genes enriched in dendrite or soma that were known binding partners of FMRP.

mRNAs that are present in dendrites at high-levels in both the ribosome-bound portion (IP) and ribosome-unbound portion (SN). To account for this we also calculated FPKM (Fragments Per Kilobase of transcript per Million mapped reads) for IP samples to capture the relative expression level for each gene within these samples. We used a

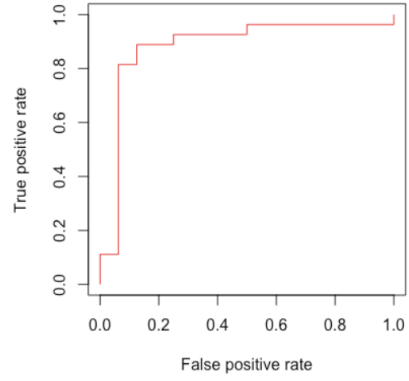
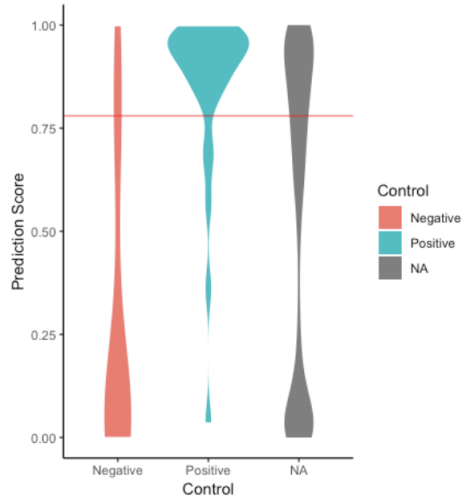
logistic regression model on our dendrite data to generate a predictive score for each gene based on the average FPKM in the IP and the log₂ fold-change between the IP and SN. The model was trained on the previously generated list of control genes and gave high predictive scores to positive control genes and low predictive scores to negative control genes (Figure 3.5A). We generated a ROC curve (Figure 3.5A) and a threshold for predictive score was chosen to optimize between false positives and false negatives. There were 2923 genes above this cut-off that were predicted to be dendritic. A subset of genes that were enriched in radiatum SN by differential expression analysis were predicted to be in dendrites based on our criteria. Among these genes was the well known dendritic marker *Map2*, validating the use of this approach (Figure 3.5B).

We compared the results of our dendritic predictions to previous dendritically localized mRNA lists (Figure 3.5C) generated by Joshua Ainsley et al. [74] and by Ivan Cajigas et al. [78]. Consistent with differences in methodology, our list did not have complete overlap with either the Ainsley or Cajigas lists, however, it is worth noting that we demonstrate more overlap with either of the previous studies than they do with each other (714 Jones-Cajigas and 478 Jones-Ainsley vs 434 Ainsley-Cajigas). The full list of dendritically predicted genes is presented in Supplementary Table 3.

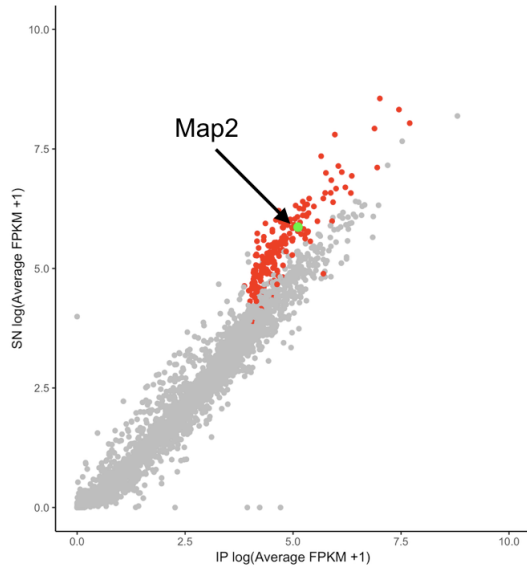
3.2 Divergent temporal dynamics of neuronal compartments after contextual fear conditioning

Recent studies have begun to use RNA-seq to probe the changes in translation that occur during memory formation [74,79,80]. These studies have so far produced

A.



B.



C.

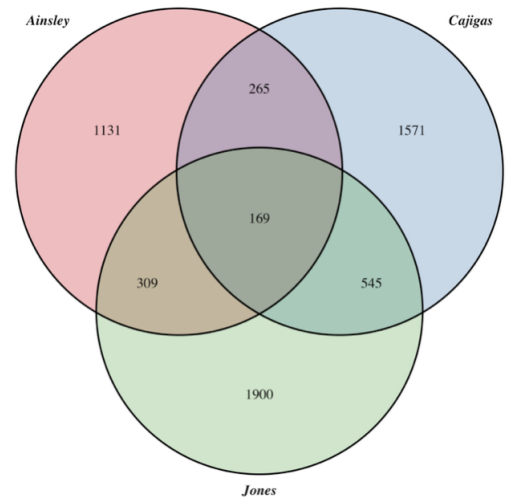


Figure 3.5 Logistic regression analysis predicts dendritically localized genes. A) A logistic regression based prediction algorithm was trained using already established control genes (see Supplemental Table 2) to generate predictive scores. Log₂ fold change estimates generated by differential expression analysis of dendrite IP and dendrite SN samples and average FPKM for each gene were used as variables in the prediction algorithm. To minimize noise, only genes which had adjusted p-value < 0.1 in the differential expression analysis were considered. Left, violin plots of positive, negative and non-control (NA) gene predictive scores. The threshold above which genes were considered to be dendritic is marked as a red bar. Right, ROC curve measuring false positive and false negative rate. B) Average IP FPKM vs Average SN FPKM for dendritically predicted genes. Genes plotted in red have negative log₂ fold changes based on differential expression, indicating a higher level of enrichment in the dendrite SN. These genes were nevertheless predicted to be dendritic based primarily on the high average IP FPKM. Dendritic marker, *Map2*, which was more enriched in dendrite SN than dendrite IP is plotted in green to emphasize the importance of including the FPKM as a measure of total expression in a sample type in the prediction algorithm. C) Venn diagram of the overlap of previously generated lists of dendritically predicted genes. Our list (Jones) has a higher degree of overlap with either of the previous lists (Ainsley, Cajigas) than they have with each other.

somewhat conflicting results. For example, Ainsley et al. found that, immediately following fear conditioning, CA1 pyramidal dendrites were enriched for ribosomes bound to mRNAs related to translation [74]. By contrast, Cho et al. found that mRNAs related to translation were repressed following fear conditioning [79]. These discrepancies likely arise due to differences in experimental design amongst the major studies that have so far been reported. To date, no study has combined cell-type and regional specificity to measure the changes that occur in translation over time during memory formation. Our experimental design (Figure 3.1B) allows us to interrogate the temporal dynamics of ribosome binding after fear conditioning in dendrites and somata.

3.2.1 TRAP greatly enhances detection of translational changes in dendrites and somata

We used DESeq2 to obtain estimated fold-changes (negative binomial Wald-test) for each behavioral time point (0 minutes, FC0; 15 minutes FC15; or 30 minutes FC30) in mice that had undergone FC compared with mice who had not had behavioral training (home cage, HC). We hypothesized that alternate pools of differentially expressed (DE) genes would be present in dendrites and somata so we therefore performed DEseq on dendrite IP and soma IP samples separately. We also separately performed DEseq on dendrite SN and soma SN samples. Dendrite samples contained 529 unique DE genes across all time points. Notably, we observed a shift from increase in ribosome binding in genes that were DE at FC0 to a decrease in ribosome binding in genes that were DE at FC15 (Figure 3.6A; FC0, 79.7% upregulated; FC15, 35.0% upregulated; FC30, 57.6% upregulated). Soma samples contained 410 unique DE genes and underwent a similar relative decrease in ribosome binding at 15 minutes but had roughly equal levels of ribosome binding increases and decreases at 0 and 30 minutes (Figure 3.6A; FC0, 57.4% upregulated; FC15, 37.2% upregulated; FC30, 55.2% upregulated). Strikingly, there were only 10 unique DE genes in dendrite SN samples. Soma SN samples contained 206 unique DE genes notably number of DE genes increased at each time point. Because the somatic micro-dissection, by definition, contains cell bodies soma SN samples are likely to include nuclear localized mRNAs and so it is likely that the increase in DE genes over the time course is due to transcriptional changes in the soma SN.

We observed very little overlap between DE genes in IP samples and SN samples

in either dendrites or somata. Only 6 genes were DE in both IP and SN of soma samples and only 1 gene was DE in both IP and SN of dendrite samples. Perhaps unsurprisingly, 50% of shared DE genes in somata and 100% of shared DE genes in dendrites were immediate early genes (IEGs) (Figure 3.6B). Immediate early genes are known to rapidly increase in expression following neuronal activity [46–48] so we expected that these genes would be upregulated at later time points in all samples. Although this was indeed the case, we noted that these expression increases were more obvious in IP samples and, as in the case of *Npas4* did not follow the same temporal dynamic in both IP and SN (Figure 3.6C).

3.2.2 Temporal patterns of alteration in ribosome binding in dendrites and somata

We wanted to further understand the temporal dynamics of differential expression at each time point in our dataset. We therefore separately performed DESeq analysis using the negative binomial likelihood ratio test to test for genes that were differentially bound to ribosomes (i.e. DE in IP) at any time-point after FC compared with HC in dendrites (Figure 3.7) and somata (Figure 3.8). The likelihood ratio test performed better for genes where very few samples in a given group were expressed at extremely high levels. We observed 206 DE genes in dendrite IP (Figure 3.7A, full list of DE genes in Supplementary Table 4) that displayed a mixture of increase and decrease in ribosome binding. In soma IP we observed 56 DE genes (Figure 3.8A, full list of DE genes in Supplementary Table 5), a substantial decrease from our results using the Wald test. There was minimal overlap in genes that were DE in both dendrite IP and soma IP. Only

Arc, *Lrrc27*, and *Fos* were significantly DE in both dendrite and somata. *Arc* and *Fos* are both IEGs and as expected follow a similar time course in both soma IP and dendrite IP (Figure 3.6C). *Lrrc27* is a member of a protein family known as leucine-rich repeat domain containing proteins many of which have a role in mediating neuronal functions including axonal guidance, synapse formation and some of which have been shown to be involved in various nervous system disorders [104].

DE genes in both dendrite IP and soma IP displayed alterations in fold-change over the time-course and we were therefore curious if these dynamics were biologically meaningful. As a first step, we performed k-means clustering to group genes by their temporal dynamics. Log₂ fold-changes at all three time-points versus HC were used to cluster significantly DE genes. To determine how many centers to use for k-means clustering, we first determined how many centers were needed before the total within-clusters sum of squares reached a lower limit (known as the “elbow method”). By chance, both dendrite IP and soma IP were optimally clustered using 4 centers (Figure 3.7B, Figure 3.8B). In dendrite IP samples, clustered genes were characterized by three prominent temporal dynamics (Figure 3.7C). The first and third clusters (as determined by the k-means algorithm) had an early increase in ribosome binding at FC0 followed by a sharp decline at FC15 and another sharp increase in ribosome binding at FC0. These two clusters differed primarily in the absolute value of fold changes. The second cluster was characterized by a sharp decrease at FC15 which rebounded to homegene levels at

Figure 3.6 TRAP improves differential expression analysis of fear conditioning time-course. A) Number of differentially expressed genes in dendrite IP and SN (left) and soma IP and SN (right) at each time-point after FC compared with HC samples. Downregulated genes are colored green, upregulated genes are colored red. B) Table of genes which were DE in both IP and SN of their corresponding samples. C) Plots of normalized gene counts for IEGs which were DE in IP and SN samples. Arc Fos and Npas4 were DE in dendrite IP, soma IP and soma SN. Fos was also DE in dendrite SN.

FC30. The fourth and final dendrite IP cluster was characterized by an increase in ribosome binding at FC15 that dropped to homecage levels by FC30. The up-down-up pattern displayed by clusters 1 and 3 appeared to be unique to dendrites. By contrast in the soma, increases (cluster 1 and cluster 4, FC0; cluster 3 FC15) or decreases (cluster 2, FC0) in ribosome binding leveled off by FC15 and did not change substantially from this level by FC30.

3.2.3 Early and intermediate ribosome binding engage alternate functions in dendrites

We were intrigued by the up-down-up pattern of ribosome binding changes in dendrite IP samples and wanted to understand if this was a function of the underlying biology. We suspected that genes exhibiting this up-down-up pattern might contribute to shared biological processes that were separate from those of genes undergoing alternate temporal dynamics. Therefore, we used The **D**atabase for **A**nnotation, **V**isualization and **I**ntegrated **D**iscovery (**DAVID**) [87] to perform functional annotation clustering of genes in different gene clusters. Because of their similar temporal dynamics we combined dendrite IP clusters 1 and 3. Cluster 2 did not return any statistically significant functional annotation clusters so we do not report gene ontology for these genes here. As

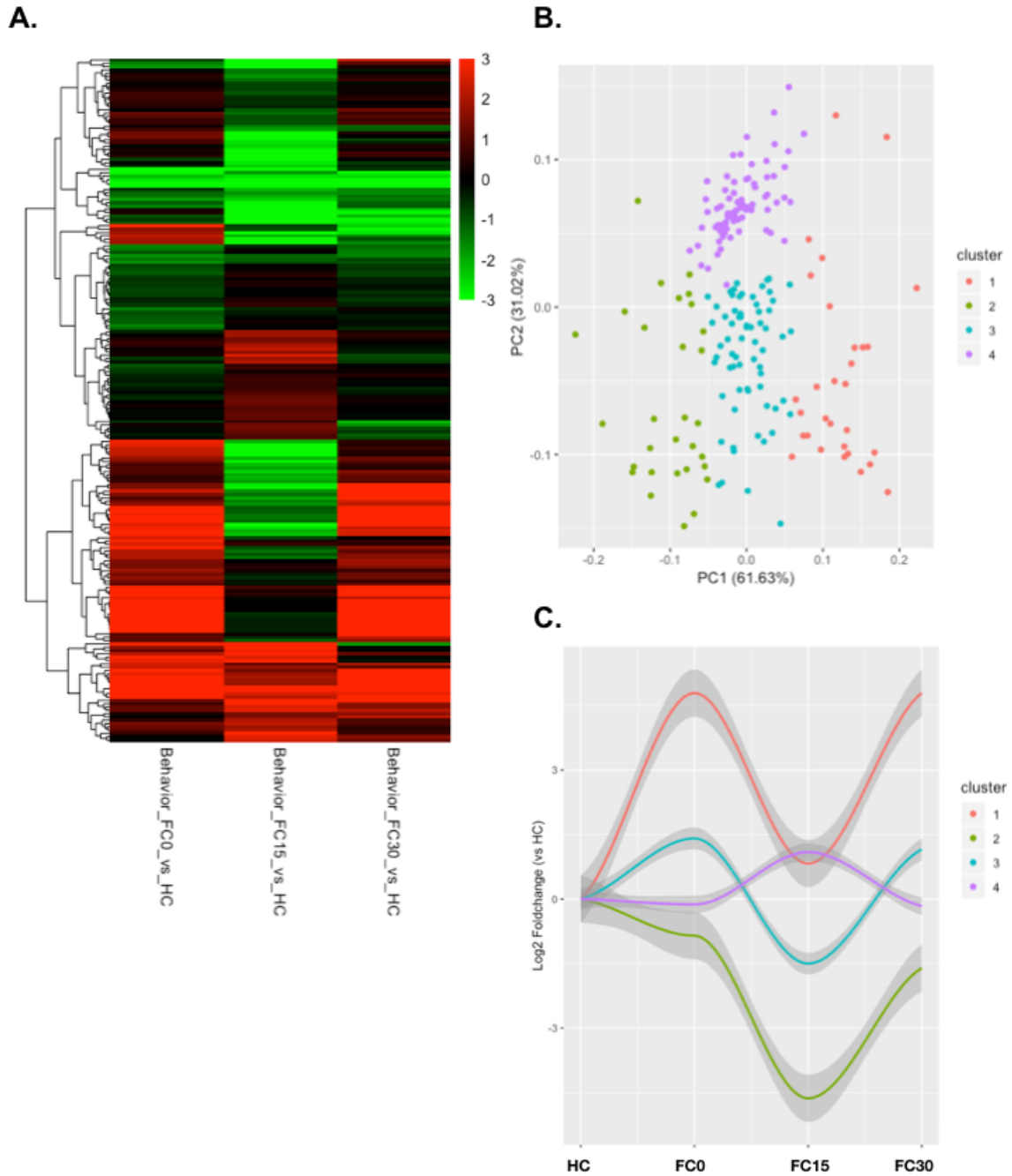


Figure 3.7 Temporal patterns of differential expressed genes in dendrite IP. A) Heatmap of all 206 significantly DE genes in dendrite IP(negative binomial likelihood ratio test, $P\text{-adj} < 0.1$). B) Principal component analysis of genes clustered by log fold change at 0, 15 and 30 minutes. Individual points correspond to single DE genes, colored by cluster. C) Plot of log fold change for each cluster. Clusters in B and C correspond to each other.

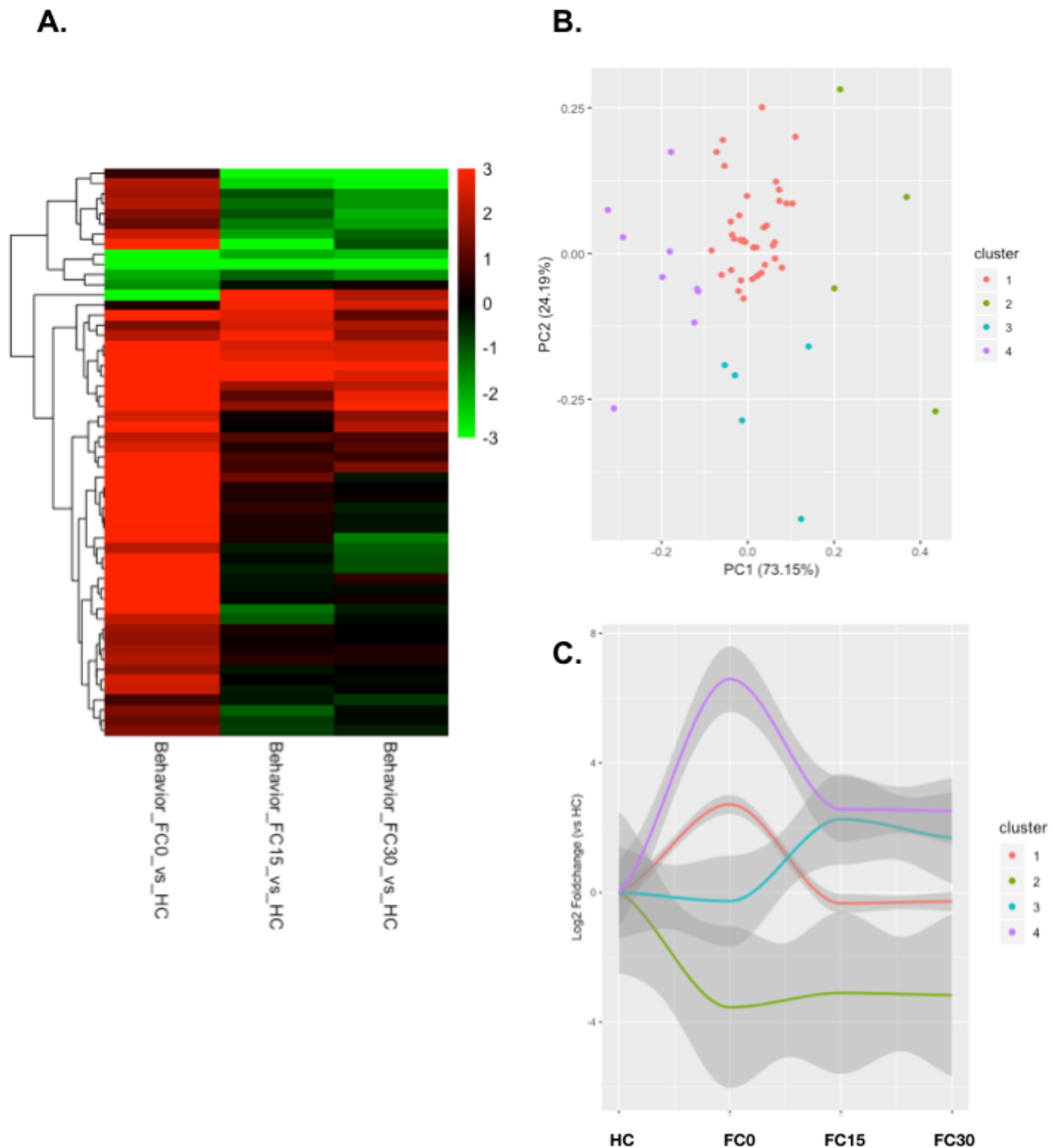


Figure 3.8 Temporal pattern of differentially expressed genes in soma IP.

A) Heatmap of all 56 significantly DE genes in soma IP (negative binomial likelihood ratio test, $P\text{-adj} < 0.1$). B) Principal component analysis of genes clustered by log fold change at 0, 15 and 30 minutes. Individual points correspond to single DE genes, colored by cluster. C) Plot of log fold change for each cluster. Clusters in B and C correspond to each other.

expected, statistically significant gene ontology terms for genes in clusters 1 and 3 varied starkly from those in cluster 4 (Figure 3.9A-B). Clusters 1 and 3 were enriched for genes associated with the membrane and its related functions (GO-term membrane accounted for 50.57% of genes in clusters 1 and 3, full list of functional annotations are provided in Supplementary Table 6). Cluster 4 was enriched for a variety of annotations with likely nuclear functions including: Cell cycle, transcription regulation and nucleotide binding (Full list of functional annotations are provided in Supplementary Table 7). Cluster 4 was also enriched for microtubule elements. Among these was the neuronal microtubule gene *Tubb3* and the immediate early gene *Arc*. Likewise, *Egr1*, *Egr4*, *Fos*, *Nr4a1* and *Nr4a2* were grouped (all immediate early genes) into the nucleotide binding annotation cluster.

Given the potentially nuclear function of a large percentage of genes in cluster for of dendrite IP samples, we wondered whether the somatic differential expression time course for these genes would provide context for how these genes came to be localized to dendrites. We hypothesized that a global increase in ribosome binding throughout the neuron could lead to a transient increase in ribosome binding within dendrites. We therefore measure fold changes for dendrite IP cluster 4 genes in soma IP samples (Figure 3.9C-D). To our surprise we found that in the soma, there is a decrease in ribosome binding at FC0 which precedes the increase in ribosome binding at FC15, suggesting that these mRNAs may begin moving into dendrites even earlier than we expect, potentially while bound to ribosomes. We also measured fold change differences for Dendrite cluster 1 and 3 genes in soma IP. Genes in these clusters initially increased in ribosome binding

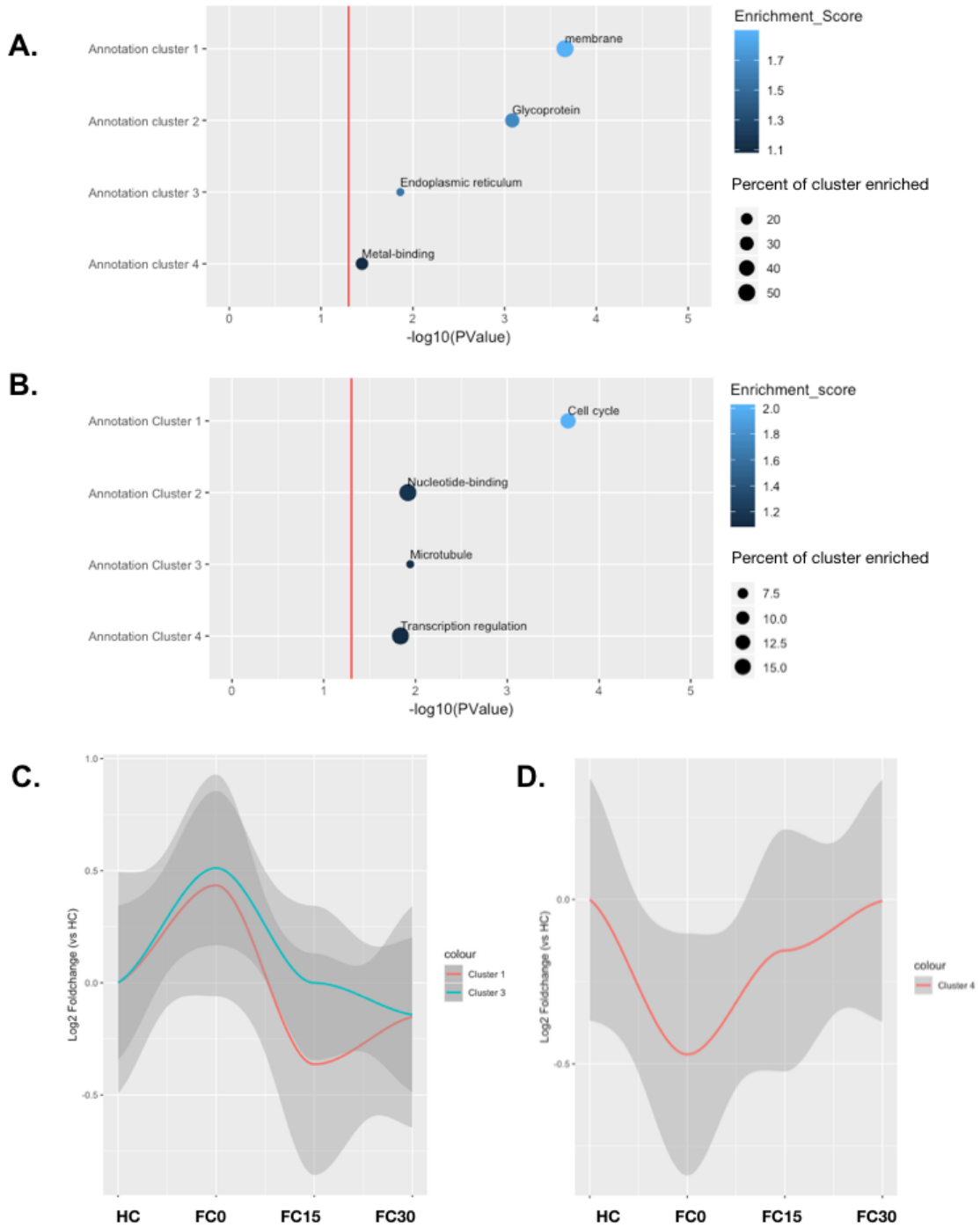


Figure 3.9 Temporally derived gene clusters are functionally distinct. A) Functional annotation clustering results for dendrite IP genes in gene clusters 1 and 3. Vertical red bar indicates a p-value of 0.05. Annotational clustering results are colored by enrichment score and sizes correspond to percentage of genes within a gene cluster that were annotated for a given term. B) Functional annotation clustering results for dendrite IP genes in gene cluster 4. C) Fold-change plots for gene clusters 1 and 3 for some IP samples. D) Fold-change plots for gene cluster 4 for some IP samples.

and had a decrease in ribosome binding at FC15, which precedes the late increase in ribosome binding that occurs in these genes in dendrite IP samples, potentially suggesting a similar translocalization of ribosome bound mRNAs into the dendrite. It is important to note that differential expression changes were not statistically significant in soma IP samples for these genes by likelihood ratio test (with the exception of *Arc*, *Lrrc27*, and *Fos*). However, because the trends are visually apparent we report these data with the aforementioned caveat.

Chapter 4: Discussion

4.1 Translational profiling of dendritic and somatically localized mRNAs

4.1.1 Prediction of dendritic mRNAs, past and present

It is clear from a vast body of work that local protein synthesis within dendrites is necessary for a variety of plasticity and memory paradigms [4,36],[19,39]. What is less clear is which plasticity mechanisms require local translation in order to properly carry out their functions. Previous studies in our lab and others[74,78,105] have worked to develop a comprehensive list of mRNAs that are locally translated within dendrites in the hope that such a list would help answer the question, “what role does local protein synthesis play during neuronal plasticity underlying learning?” Here we add to this body of work and produce our own list of predicted dendritic mRNAs. Notably, we achieve greater overlap between our list and either of two previous lists than those lists had with each other (Figure 3.5C). Our data thus add further support for these previous studies (Ainsley et al.[74] and Cajigas et al.[78]). We also propose an additional 1900 genes not previously predicted to be in dendrites. It is not surprising that complete overlap with the Ainsley or Cajigas dendritic predictions was not observed. Lack of overlap can be readily explained by differences in experimental design. Cajigas et al. generated dendritic predictions by first collecting total mRNA isolated from stratum radiatum and ensured neuronal specificity of their predictions by filtering genes that were previously found to be expressed in non-pyramidal cell-types, as well as genes with a known nuclear function. Ainsley et al. ensured cell-type specificity with the same TRAP methodology used in our study and were therefore able to predict dendritically localized mRNAs that

had been filtered from the Cajigas list. Importantly, TRAP specifically isolates ribosome bound mRNAs. Although it is possible that a subset of mRNAs pulled down using this technique are stalled, it is worth noting that the majority of translational regulation occurs at the initiation step [7,16] and even mRNAs bound to single ribosomes, long thought to be the products of stalled translation, actively contribute to synthesis of proteins at low levels [106]. TRAP is therefore more likely to reveal genes which are part of an actively translated pool of mRNAs rather than simply mRNAs which arrive in the dendrites as a result of “spill-over” localization from somata.

To generate their list, Ainsley et al. employed a machine learning algorithm based on support vector machines which used two separate expression values for each gene; one for the coding sequence and 3'UTR adjacent to the stop codon and one for the distal 3'UTR. Splitting the data in this way was done to account for loss of coverage in distal 3'UTR of RNA-seq reads in the IP due to RNA fragmentation. Given the greater numbers of biological samples from which our dendritic predictions were based and the lack of a clear trend indicating fragmentation of the RNA and loss of 3'UTR coverage in IP samples (data not shown) we decided not to employ this approach and to instead base our predictions on enrichment of genes in the IP samples (versus SN) and total expression in the IP samples for each gene. Differences in dendritic gene lists are also likely to be due to the inclusion of later fear conditioning time-points included in our analysis. Our list of dendritic predictions therefore represents mRNAs that are possibly localized to CA1 dendrites and bound to ribosomes at any point prior to and up to 30 minutes following neuronal activation by contextual fear conditioning. Although it is the largest list of

dendritically predicted mRNAs to date, it should by no means be considered exhaustive. In order to reduce noise produced by unreliable fold changes in our dendritic predictions we only considered genes that were significantly differentially expressed between IP and SN in dendrite samples. Thus a limitation of our approach is that there were mRNAs that we detected in our dendritic microdissection at roughly equivalent levels in both the IP and SN, but that we cannot predict as being truly dendritic using our current method. Future work in our lab will focus on refining our prediction algorithm.

4.1.2 Implications of dendritic mRNA diversity for synaptic plasticity mechanisms

The dendritic compartment is a spatially limited region of the neuron that, based on imaging data [107] and measurements of mRNA copy abundance in other cell-types [108,109], likely contains an order of magnitude fewer mRNA transcripts than does the neuronal cell body [95]. As argued by Kenneth Kosik, roughly 100,000 mRNA copies are split amongst the pool of dendritically localized mRNA pool. Kosik suggests that these 100,000 mRNAs are split amongst the roughly 2500 genes found to be dendritically predicted in the Cajigas list. Kosik further suggests there are approximately 500 copies of the 100 most abundant genes and roughly 21 copies each of the less abundant genes based on observations from single cell RNA-sequencing of rat pyramidal neurons [110]. However, as our data and previous work in our lab show, the actual number of dendritically localized genes is likely to be much larger than suggested by Cajigas. Integrating the Ainsley and Cajigas lists with our own, the true number of dendritically localized mRNAs is potentially as large as roughly 6000 genes or more. Following the

same logic used by Kosik to generate these approximations, there are thus potentially as few as 9 copies of each of the least abundant mRNAs. Given the low amount of overlap in gene profiling studies it seems likely that more dendritically localized mRNAs will be predicted, potentially pushing low abundance mRNAs to a vanishingly small approximate number of copies present within each dendritic arbor if Kosik's model holds. On the other hand it is possible that dendritically localized genes are present in individual dendrites at variable rates. High throughput screens using bulk RNA such as ours cannot differentiate between individual neurons and most single-cell RNA sequencing methods require enzymatic dissociation that remove neuronal processes making it impossible to use these methods to study local translation within the dendrites of a single neuron. However, some evidence that individual dendrites express different subsets of genes is provided by a recent study from Sarah Middleton, James Eberwine and Junhyong Kim [111]. They used a sub-cellular sequencing approach to sequence individual dendrites and somata from single neurons and observed a subset of "high variability" dendritically localized mRNA that were expressed in an "all or nothing" pattern from cell to cell. Such high variability genes may come about as a result of differences in activity dependent localization of specific mRNAs between individual neurons over the lifetime of those cells resulting in a recruitment of unique pools of mRNAs to individual dendritic arbors, akin to a "dendritic fingerprint".

Along these lines, our data revealed a greater diversity of ribosome bound mRNAs enriched in dendrites than in somata (3,037 genes enriched in dendrite IP vs 1,179 enriched in soma IP; Figure 3.3) suggesting a greater degree of heterogeneity

among dendrites than somata. This trend was not mirrored in SN samples, suggesting that heterogeneity amongst IP samples was specific for subcellular compartments and not merely regional. Additionally, because this trend was observed in the ribosome-bound IP portion indicating a greater likelihood that these mRNAs would be translated, it is likely to be functionally relevant. The implication of these results is that dendritic heterogeneity is not simply a result of individual cell to cell variability but rather it is the result of functional differences between the two cellular compartments. One possibility is that dendritic heterogeneity may arise as a consequence of differences in activity at specific synapses. This interpretation of our data is consistent with the synaptic tagging model which proposes that activated synapses are “tagged” in a protein synthesis independent manner which allows these synapses to then “capture” plasticity related products (PRPs) [112,113]. PRPs might include proteins synthesized in the somata or mRNAs which are then transported to tagged synapses. Although our study does not directly address whether dendritically enriched genes are distributed to specific synapses, there is evidence that that is likely to be the case. One of the most abundant types of genes predicted to be dendritic in our dataset and others are those which encode cytoskeletal proteins and other structural elements. These genes contribute to the structural plasticity that occurs following synaptic activity and allows for the growth of new dendritic spines and the enlargement of existing ones in a synapse-specific manner [114,115]. A recent study by Jun-Hyeok Choi et al. found that contextual fear conditioning induced an increase in size and number of synapses that was correlated to the strength of the fear conditioning protocol used and thus to the retrieval of that fear

memory [116]. Thus structural remodeling of synapses driven by translation of cytoskeletal proteins give rise to a “synaptic engram” the strength of which is correlated with the strength of the memory. It may also be the case that other classes of genes aside from cytoskeletal are involved in the formation of synaptic engrams. Within our dataset, low abundance mRNAs that are nevertheless predicted to be localized to dendrites are likely to be localized selectively to individual dendritic branches or synapses rather than constitutively throughout the stratum radiatum. Such genes would be good candidates for future studies that attempt to further resolve the mechanisms by which synaptic engrams may arise.

4.1.3 Regulatory features associated with Dendritic mRNAs

Of great interest among those studying local translation is how this system is regulated and how those mechanisms differ from those employed constitutively within the whole neuron. Neurons can selectively target mRNAs to their processes but it is not clearly understood how this occurs. A well known example of this is seen in the neurotrophin, BDNF. Two isoforms of BDNF mRNA are produced in the brain, that vary based on their 3'UTR length. The short 3'UTR version of BDNF is restricted to the somata while the long 3'UTR isoform is trafficked into dendrites in an activity dependent manner [99,117]. Likewise, as mentioned previously, a dendritic targeting element (DTE) within the 3'UTR of the mRNA for *Camk2a* was first identified in 1996 by Mayford et al [38]. A handful of other genes have also been found to contain DTEs within their 3'UTRs including MAP2, Arc and Shank1 [118–120] However, these DTEs do not contain

significant sequence similarity to each other, making prediction of other DTEs difficult. It is possible that protein interactions with the secondary structure of the DTE sequence are ultimately what drives localization of genes containing these features into the dendrites. DTEs can range from a couple hundred base pairs long to multiple kilobases (as is the case with BDNF). Our data showed that ribosome-bound mRNA enriched in dendrites had longer average 3'UTRs as compared with ribosome bound mRNA enriched in somata (Figure 3.4). It is likely the case that several of these mRNAs contain previously undiscovered DTEs. Notably this trend was reversed in comparison of SN samples. That is, mRNAs enriched in dendrite SN samples in our dataset had significantly shorter 3'UTRs as compared with those enriched in soma SN samples. Because soma SN samples are likely to be much more enriched in mRNAs originating from neurons due to a greater density of cells and more homogeneity of cell-type within the stratum pyramidale, this data supports studies that have shown a preference for longer 3'UTR isoforms in neuronal cells [96]. In fact, the trends present in the 3'UTR in comparisons between dendrite and soma samples were mirrored in the 5'UTR. This finding is consistent with the idea that neurons, as highly specialized cells, require multiple strategies to regulate translation, many of which rely on the presence of motifs within the primary or secondary sequence for interactions with RNA binding proteins or miRNAs.

In previous studies of local translation, translation has been consistently found to be among the most highly enriched gene ontology (GO) terms [74,121,122]. Although translation was not among the top enriched GO terms in our data set, several genes known to be a part of the translational machinery were enriched in dendrite IP samples as

compared with soma IP samples including three genes which encode ribosomal subunits (*Rpl19*, *Rpl18*, *Rps15a*). While it makes intuitive sense that translational machinery might need to be translated locally given that quickly putting that translational machinery to work following synaptic activity seems to be a key design element of dendrites, ribosomes have not yet been shown to be capable of *de novo* assembly outside of the nucleolus. Nevertheless, this finding is consistent with earlier findings in our lab which also found ribosomal protein mRNAs to be predicted in dendrites [74]. There are several possible scenarios which may explain why ribosomal protein mRNAs are localized to dendrites. First, it is possible that ribosomes, in fact, are assembled *de novo* within dendrites or that subunits may be swapped out as necessary to prolong the lifespan of already assembled ribosomes. A second possibility is that ribosomal protein mRNAs are localized to dendrites incidentally by the same pathway which localizes other translational machinery mRNAs to dendrites. Indeed many of the translational machinery genes contain 5' TOP motifs and are commonly regulated by mTORC1 [9,14]. We show that there is a modest enrichment for TOP motif containing genes in the dendrite IP compared with the soma IP samples (Figure 3.4). It has been suggested that local synthesis of TOP motif containing mRNAs may be important for synaptic plasticity by increasing the overall translational capability within dendrites [123]. It is possible that the TOP motif itself or some other feature shared amongst TOP-motif containing mRNAs also regulates their localization, though no such mechanism has yet been found. On the other hand, more than half of the known TOP motif containing genes (60 of 109) were enriched in dendrite SN compared with only 2 TOP genes in the soma SN (Figure 3.4).

This could indicate that TOP genes are enriched in non-neuronal cells within the stratum radiatum or that these mRNAs were simply localized to dendrites but not bound to ribosomes. While our data cannot differentiate between these two possibilities, given the available evidence suggesting that local protein synthesis of TOP genes is involved in synaptic plasticity and the dearth of TOP genes in both the soma IP and soma SN samples it seems likely that some mechanism exists to specifically shuttle TOP genes into the dendrite. The final possibility is that the ribosomal proteins synthesized within dendrites have a function that is completely separate from their role within ribosomes. Several ribosomal proteins have, for example, been found to activate the pro-apoptotic tumor suppressor p53 pathway [124,125]. Some research has suggested that moderate activation of pro-apoptotic genes may aid in synaptic plasticity. For example Mattson and Duan found that caspase activation could lead to degradation of glutamate receptor subunits, leading to a reduced glutamatergic response [126]. Importantly, none of these three possibilities are mutually exclusive and it could be that all or some combination of these occurs.

Among the genes that were DE between dendrite IP and soma IP, we saw that nearly ~8% of genes enriched in the dendrite IP were FMRP targets compared with only about ~5% of genes enriched in soma IP that were FMRP targets (a 1.5X enrichment). FMRP-mRNA binding is thought to mediate two separate functions, repression of mRNA translation and localization of mRNAs into the dendrites [127,128]. Because FMRP is thought to repress translation at the elongation phase, repressed mRNAs might still be present in our ribosome bound IP samples[129]. Conversely, release of FMRP repression

could have the effect of reducing the enrichment of these genes in IP samples if, for example, these genes are stalled in large numbers such that when repression was released, and protein synthesis was successfully completed, ribosomes were able to dissociate from the mRNA causing it to leave the IP and enter the SN mRNA pool. Notably, FMRP is known to not be required for dendritic localization of all of its targets [130]. Our system provides an ideal method by which to test both dendritic targeting and translational repression of FMRP target candidate genes. An active area of research being pursued in our lab utilizing the same dendrite TRAP approach described here in an FMR-KO x Camk2a-EGFP-L10a mouse line. The groundwork we have laid here has established a list of candidate genes (247 FMRP targets that were enriched in dendrite IP samples vs 98 in soma IP) that we will test for perturbations in our future study.

4.2 Temporal dynamics of protein translation during memory

4.2.1 Advantages of TRAP for studying changes in local translation over time

One of the major takeaways from the early studies of protein translation using protein synthesis inhibiting drugs was this: timing is everything. Application of protein synthesis inhibitors prior to training can block long-term but not short term memory [4]. However, even the short span of time during which an animal is undergoing behavioral training can be enough for protein synthesis to occur, allowing long term memories to be stored. Administration of anisomycin 15 minutes prior to training but not administration immediately following behavioral training was capable of blocking long term memory up to one week later [131,132]. In fact, multiple rounds of protein synthesis occur and

support long term memory. Blocking protein synthesis at 12 or 24 hours after behavioral training has been shown to impair memory retention [131]. IEGs are another well known example of temporal dynamics in gene expression changes that occur after neuronal activity. Indeed, it is hard to imagine a scenario in which careful temporal regulation of protein synthesis does not occur at a fine level, occurring in multiple waves of translation over the course of minutes to hours following learning. The alternative, in which translation increases constitutively, might quickly burn up translational resources (translational machinery, free amino acids and ATP) especially in spatially limited regions such as dendrites where such resources may be scarce or and would reduce the capacity for tight spatial and temporal regulation of signaling cascades that are required for cellular function. In order to gain a complete understanding of how memories are formed and stored at the molecular level, it is thus imperative that we have a full picture of the translational dynamics in the minutes and hours following learning.

Recent studies have made attempts to address this challenge and have come to surprisingly disparate conclusions. In our lab, Ainsley et al. captured the ribosome binding profiles of CA1 dendrites immediately after fear conditioning and observed widespread ribosome binding increases [74]. In contrast, Cho et al. used ribosomal footprint analysis of whole hippocampus to show that during the early time course after fear conditioning, translational repression dominated the changes in differential expression [79]. There were a few major differences between these two studies. 1) Ainsley et al used TRAP to isolate their mRNA in a cell-type specific way to analyze dendritically localized genes whereas Cho et al. collected mRNA from whole

hippocampus which contains a mixture of excitatory neurons, interneurons and glial cells. Thus the gene expression profiles of these two studies were very different and may have represented different cell types. 2) Cho et al collected mRNA at 5 minutes, 10 minutes, 30 minutes and 4 hours after fear conditioning. Ainsley et al. collected mRNA immediately after fear conditioning but did not collect any mRNA at later time points. In our study, we included two additional time points (0 minutes, 15 minutes and 30 minutes following fear conditioning) which allow us to better compare our cell-type specific approach with the study from Cho et al.

The advantages of a TRAP-based cell-type specific approach are immediately apparent in the dendrite (Figure 3.6). In dendrite SN samples only 10 genes were differentially expressed. The neuropil which makes up the stratum radiatum, from which these mRNA samples were collected, is a heterogeneous mixture of dendritic and axonal processes from CA1 and CA3 respectively as well as glial and interneuronal cell-types. It is probable that other cell-types contained within the stratum radiatum undergo activity dependent changes in translation, potentially over the same time course in which we collected mRNA. For example, interneurons have been shown to respond to neuronal activity by modulating the expression of transcriptional regulator Er81 [133]. Likewise astrocytes locally translate mRNAs within their peripheral processes [63] and it is possible this translation is modulated by activity to some degree. However, those changes are masked by the high levels of background mRNA in the dendrite SN. In the soma, where mRNA was collected from the more cellularly homogeneous stratum pyramidale, gene expression changes are more obvious. Despite this fact, only 6 genes were

differentially expressed in both IP and SN of Soma, 50% of which were IEGs. In addition, IP samples had twice the number of differentially expressed genes (410 soma IP versus 206 soma SN) demonstrating the utility of our model. As a separate measure to assess the quality of our data, we compared DE genes in our dendrite dataset (Supplementary Table 4) with a list of non-neuronally enriched genes generated using the Brain RNA-seq dataset generated by Ye Zhang et al. [134] and found that the majority of DE genes did not appear to be enriched in non-neuronal cell-types. However, of the list of ~200 most highly DE genes 11 were included in the list of non-neuronally enriched (*Abcb1a*, *Atf3*, *Enpp6*, *Lyl1*, *Pdgfd*, *Pla2g4a*, *Rcsd1*, *Sema3g*, *Snx20*, *Sox17* and *Tie1*) corresponding to about a 5% false positive rate. On the other hand, Ye Zhang et al did not perform any behavioral assays on mice prior to collection of specific cell-types so it is possible that these genes appear in our dataset only in response to neuronal activity. An illustration of this is the gene *Atf3* which is DE in our dendrite dataset, as well as apparently enriched in non-neuronal cell types. Patrick Chen et al. found *Atf3* to be significantly upregulated in hippocampal CA1 neurons in response to NMDA receptor dependent late-LTP [80,134]. Likewise, long-term memory is mediated in an NMDA receptor-dependent manner [135–138]. It is therefore likely that at least some supposedly non-neuronally enriched genes found in our dataset are included due to the activity-dependent regulation of those genes.

Nevertheless, our data add evidence to support a wide-spread repression of translation after fear conditioning. Our data suggest an additional detail of this model. The majority of ribosome binding changes occurring in our data set were increases until

15 minutes after fear conditioning. Therefore repression appears to predominate at some point between immediately after fear conditioning (when we noticed an increase in ribosome binding) and 5 minutes after fear conditioning (the first time point for which mRNA was collected in Cho et al.). We observe this for both dendrite IP and soma IP samples, though the effect was stronger among dendrites. This finding bridges the conceptual gap between Ainsley et al and Cho et al. Although we cannot rule out the possibility that ribosome binding of mRNAs is increased at FC0 and then immediately paused during elongation, such a finding would be interesting in its own right given that the majority of translational regulation is accomplished at the level of initiation [9,16] and would suggest that this method of translational control is more common than expected.

4.2.2 Multiple waves of protein synthesis in dendrites after learning

The idea that multiple waves of protein synthesis are necessary for memory has been around since the early 2000's. As described above, protein synthesis inhibitor studies made clear that the initial round of protein synthesis after learning is followed by a required second round of protein synthesis in the hours that follow [131,132,139]. In this study we show a much more rapid temporal pattern in which multiple waves of protein synthesis are carried out within minutes of each other. In Figure 3.9 we clustered genes that were DE compared to HC at 0, 15 or 30 minutes after FC based on their fold changes. Interestingly, both dendrite IP and soma IP DE genes clustered into separate temporal patterns but only genes that were DE in dendrite IP displayed early (0 minute)

and late (30 minute) waves of ribosome binding increases within a single set of genes. These ribosome binding increases were separated by a decrease in ribosome binding at 15 minutes that was at or below ribosome binding levels in HC mice. This up-down-up temporal pattern contributed to different cellular functions as described by gene ontology than did genes that increased in ribosome binding specifically at 15 minutes following fear conditioning (Figure 3.9). Specifically, 50% of up-down-up genes were enriched for GO terms related to membrane, including a subset which were annotated as having transmembrane domains (Supplementary Table 6). In order to be functional once translated, transmembrane proteins must be co-translationally shuttled into the endoplasmic reticulum. In keeping with this idea, studies have shown activity dependent modulation in endoplasmic reticulum structure within dendrites [140]. Although endoplasmic reticulum within dendrites tends to be smooth endoplasmic reticulum with relatively sparse ribosomes [141], this is in agreement with the relatively sparse number of total mRNA copies in a given dendrite [95] Indeed this sparseness is consistent with the early-late pattern of these genes in our dataset. Our data would predict a model in which ribosomes and associated translocons are rapidly used up following fear conditioning and are subsequently replaced within 30 minutes, either through remodeling of the endoplasmic reticulum to recruit this molecular machinery from neighboring synapses or else translocation of these proteins from somata.

A large cluster of genes in our dataset increased in ribosome binding at FC15 within dendrite IP samples. Although a smaller percentage of these genes had statistically significant GO terms associated with them (Supplementary Table 7), those that did had

functions most often associated with the nucleus (e.g. cell cycle, nucleotide-binding, transcription regulation, Figure 3.9B). It's possible that these genes represent "spill-over" from the somatic compartment into the dendrite and we cannot rule that out in our study. On the contrary, a corresponding (though not statistically significant) dip in ribosome binding in soma IP precedes the increase in ribosome binding observed in dendrite IP which may be the result of translocation of these ribosome bound mRNAs into dendrites. Spill-over and unnecessary translation of genes meant for a nuclear fate may be merely a side-effect of global increase in translation of these genes and could have one of three consequences. 1) It may siphon off translational resources in the dendrite providing a negative feedback mechanism in order to keep noise low, while the nuclear protein itself goes unused and is ultimately degraded. 2) Conversely, spill-over mRNAs may dissociate from ribosomes and be degraded, replenishing translational machinery rather than using it up. Several of the genes in this cluster are IEGs whose expression is tightly regulated both at the protein and mRNA level [142]. Such mRNAs are rapidly targeted for degradation, for example by microRNAs, freeing up their ribosomes. 3) Finally, it is possible that some of these genes have functions other than their known nuclear functions.

One enticing possibility is that up-down-up genes, especially those with functions at the membrane, may be translational correlates of the "synaptic engram" described above. If such synaptic engrams existed, they would require insertion of membrane bound proteins at the synapse to help strengthen connectivity between pre-and-post synapse as well as to modulate the signaling capacity via insertion of receptors and ion

channels. In this cluster of genes within our data set there are several already known to have functions at the synapse, including the leucine rich repeat protein gene *Lrrtm4* which mediates excitatory synapse development [143], *Grip1* which colocalizes with inhibitory synapses [144] and synaptic organizing protein, *Agrn* which plays a role in stabilizing the post-synapse in response to destabilization by acetylcholine [145]. Other genes in our dataset that cluster into this up-down-up category are therefore good candidates to further explore how local protein synthesis contributes to synaptic plasticity and memory.

4.3 Future Directions

The data presented here lay the groundwork for a generation of future experiments in our lab and, we hope, the field at large. That said, there are several future studies which are of immediate interest to us and I will describe them briefly here. First, our study thus far has been entirely gene-level, however a primary advantage of RNA-seq over microarray is that reads are sequenced in an unbiased way providing access to information about what isoforms are present in the sample. For example, we have searched for differences in several gene-level modes of regulation amongst the gene clusters we describe in this study, including 5'UTR and 3'UTR length, presence of TOP-motifs or upstream open reading frames and microRNA binding sites (data not shown) and have so far found no statistically significant features that would explain variations in temporal pattern. Key regulatory features in these genes, may not be encoded in the exon for these genes however. Studies have shown that intronic sequences can target

cytoplasmic mRNAs into dendrites [146]. One recent study by Sharangdhar et al showed that a retained intron mediated localization of *Calm3* mRNA into the dendrites via interaction with the RNA binding protein Staufen2 [147]. By comparing intron retention in mRNA in dendrite IP samples with dendrite SN and soma IP and SN samples we may be able to identify more such intronic localization sequences.

Second, given the dendritic localization and translational repression functions of FMRP, and its relevance to human disease, our lab has begun collecting mRNA from dendrite and soma dissections in Camk2a-TRAP mice crossed with FMR knock-out mice. Our data indicate the presence of 247 FMRP targets within dendrites, but as mentioned above, not all of FMRP's targets require it for dendritic localization. By comparing our current data set with the FMR-KO data set we should be able to better understand which mRNAs require FMRP in order to localize to dendrites. Furthermore, perturbations of local protein synthesis in FMR-KO mice may be interesting in their own right, providing insight into abnormalities in structural plasticity that occur in Fragile X [127]. Indeed, if genes clustered into up-down-up temporal patterns are truly important for anything approaching a synaptic engram, their tight temporal regulation is likely to be altered in the FMR-KO data in which dendritic spine abnormalities are common.

Finally, it will be important to validate our findings with regard to the temporal pattern of local translation at the protein level. Such experiments may be conceptually easiest to perform in cell culture where single dendrite resolution may be achieved for imaging. Techniques such as SINAPS (Single-molecule imaging of nascent polypeptides) recently developed in Robert Singer's lab [148] allow translation dynamics to be tracked

directly for single mRNAs by fluorescent reporter. Such an approach is ideal for confirming temporal dynamics of translation for target candidates identified in our study.

4.4 Concluding remarks

We present this work in the hope that it will add to our understanding of how memory is formed and ultimately stored at a molecular level. This translational profiling approach has identified new candidates for genes that may potentially be [131] dendritically translated and has furthered our understanding of certain regulatory features borne by those candidate genes. Our study has also revealed a previously unknown temporal dynamic of ribosome binding during the first 30 minutes after a learning paradigm. These findings lay the groundwork for future studies in which we will hopefully be able to directly test the necessity of candidate genes and pathways by genetic perturbation of upstream regulators (as in the case of FMRP target genes) or of the candidate genes themselves.

Chapter 5: References

1. Cajal SRY. The Croonian Lecture: La Fine Structure des Centres Nerveux. *Proc R Soc Lond.* 1894;55: 444–468.
2. Yarmolinsky MB, G L D. INHIBITION BY PUROMYCIN OF AMINO ACID INCORPORATION INTO PROTEIN. *Proceedings of the National Academy of Sciences.* 1959;45: 1721–1729.
3. Flexner JB, Flexner LB, Stellar E. Memory in Mice as Affected by Intracerebral Puromycin. *Science.* 1963;141: 57–59.
4. Davis HP, Squire LR. Protein synthesis and memory: a review. *Psychol Bull.* 1984;96: 518–559.
5. Kelleher RJ 3rd, Govindarajan A, Jung H-Y, Kang H, Tonegawa S. Translational control by MAPK signaling in long-term synaptic plasticity and memory. *Cell.* 2004;116: 467–479.
6. Costa-Mattioli M, Gobert D, Harding H, Herdy B, Azzi M, Bruno M, et al. Translational control of hippocampal synaptic plasticity and memory by the eIF2alpha kinase GCN2. *Nature.* 2005;436: 1166–1173.
7. Costa-Mattioli M, Sossin WS, Klann E, Sonenberg N. Translational control of long-lasting synaptic plasticity and memory. *Neuron.* 2009;61: 10–26.
8. Dever TE. Gene-Specific Regulation by General Translation Factors. *Cell.* 2002;108: 545–556.
9. Costa-Mattioli M, Sonenberg N, Klann E. Translational Control Mechanisms in Synaptic Plasticity and Memory. *Learning and Memory: A Comprehensive Reference.* 2008. pp. 675–694.
10. Mathews M, Sonenberg N, Hershey JWB. *Translational Control in Biology and Medicine.* CSHL Press; 2007.
11. Iacono M, Mignone F, Pesole G. uAUG and uORFs in human and rodent 5' untranslated mRNAs. *Gene.* 2005;349: 97–105.
12. Haghghat A, Mader S, Pause A, Sonenberg N. Repression of cap-dependent translation by 4E-binding protein 1: competition with p220 for binding to eukaryotic initiation factor-4E. *EMBO J.* 1995;14: 5701–5709.
13. Pause A, Belsham GJ, Gingras A-C, Donzé O, Lin T-A, Lawrence JC, et al. Insulin-dependent stimulation of protein synthesis by phosphorylation of a regulator of 5'-cap function. *Nature.* 1994;371: 762–767.
14. Thoreen CC, Chantranupong L, Keys HR, Wang T, Gray NS, Sabatini DM. A unifying model for mTORC1-mediated regulation of mRNA translation. *Nature.* 2012;485: 109–113.
15. Banko JL, Hou L, Klann E. NMDA receptor activation results in PKA- and ERK-dependent Mnk1 activation and increased eIF4E phosphorylation in hippocampal area CA1. *J Neurochem.* 2004;91: 462–470.
16. Kelleher RJ 3rd, Govindarajan A, Tonegawa S. Translational regulatory mechanisms in persistent forms of synaptic plasticity. *Neuron.* 2004;44: 59–73.
17. Tsokas P. Local Protein Synthesis Mediates a Rapid Increase in Dendritic Elongation

- Factor 1A after Induction of Late Long-Term Potentiation. *Journal of Neuroscience*. 2005;25: 5833–5843.
18. Bradshaw KD, Emptage NJ, Bliss TVP. A role for dendritic protein synthesis in hippocampal late LTP. *Eur J Neurosci*. 2003;18: 3150–3152.
 19. Huber KM, Kayser MS, Bear MF. Role for rapid dendritic protein synthesis in hippocampal mGluR-dependent long-term depression. *Science*. 2000;288: 1254–1257.
 20. Sajikumar S, Frey JU. Late-associativity, synaptic tagging, and the role of dopamine during LTP and LTD. *Neurobiol Learn Mem*. 2004;82: 12–25.
 21. Gallagher SM. Extracellular Signal-Regulated Protein Kinase Activation Is Required for Metabotropic Glutamate Receptor-Dependent Long-Term Depression in Hippocampal Area CA1. *Journal of Neuroscience*. 2004;24: 4859–4864.
 22. Waung MW, Pfeiffer BE, Nosyreva ED, Ronesi JA, Huber KM. Rapid Translation of Arc/Arg3.1 Selectively Mediates mGluR-Dependent LTD through Persistent Increases in AMPAR Endocytosis Rate. *Neuron*. 2008;59: 84–97.
 23. Yilmaz-Rastoder E, Miyamae T, Braun AE, Thiels E. LTP- and LTD-inducing stimulations cause opposite changes in arc/arg3.1 mRNA level in hippocampal area CA1 in vivo. *Hippocampus*. 2010;21: 1290–1301.
 24. Steward O, Wallace CS, Lyford GL, Worley PF. Synaptic activation causes the mRNA for the IEG Arc to localize selectively near activated postsynaptic sites on dendrites. *Neuron*. 1998;21: 741–751.
 25. Wu L, Wells D, Tay J, Mendis D, Abbott MA, Barnitt A, et al. CPEB-mediated cytoplasmic polyadenylation and the regulation of experience-dependent translation of alpha-CaMKII mRNA at synapses. *Neuron*. 1998;21: 1129–1139.
 26. Wells DG, Richter JD, Fallon JR. Molecular mechanisms for activity-regulated protein synthesis in the synapto-dendritic compartment. *Curr Opin Neurobiol*. 2000;10: 132–137.
 27. Bear MF, Huber KM, Warren ST. The mGluR theory of fragile X mental retardation. *Trends Neurosci*. 2004;27: 370–377.
 28. Huber KM, Gallagher SM, Warren ST, Bear MF. Altered synaptic plasticity in a mouse model of fragile X mental retardation. *Proceedings of the National Academy of Sciences*. 2002;99: 7746–7750.
 29. Bodian D. A SUGGESTIVE RELATIONSHIP OF NERVE CELL RNA WITH SPECIFIC SYNAPTIC SITES. *Proceedings of the National Academy of Sciences*. 1965;53: 418–425.
 30. Steward O, Levy WB. Preferential localization of polyribosomes under the base of dendritic spines in granule cells of the dentate gyrus. *J Neurosci*. 1982;2: 284–291.
 31. Rao A, Steward O. Evidence that protein constituents of postsynaptic membrane specializations are locally synthesized: analysis of proteins synthesized within synaptosomes. *J Neurosci*. 1991;11: 2881–2895.
 32. Weiler IJ, Greenough WT. Potassium ion stimulation triggers protein translation in synaptoneurosomal polyribosomes. *Mol Cell Neurosci*. 1991;2: 305–314.
 33. Torre ER, Steward O. Demonstration of local protein synthesis within dendrites

- using a new cell culture system that permits the isolation of living axons and dendrites from their cell bodies. *J Neurosci.* 1992;12: 762–772.
34. Feig S, Lipton P. Pairing the cholinergic agonist carbachol with patterned Schaffer collateral stimulation initiates protein synthesis in hippocampal CA1 pyramidal cell dendrites via a muscarinic, NMDA-dependent mechanism. *J Neurosci.* 1993;13: 1010–1021.
 35. Dieterich DC, Hodas JLL, Gouzer G, Shadrin IY, Ngo JT, Triller A, et al. In situ visualization and dynamics of newly synthesized proteins in rat hippocampal neurons. *Nat Neurosci.* 2010;13: 897–905.
 36. Kang H, Schuman EM. A Requirement for Local Protein Synthesis in Neurotrophin-Induced Hippocampal Synaptic Plasticity. *Science.* 1996;273: 1402–1406.
 37. Vickers CA, Dickson KS, Wyllie DJA. Induction and maintenance of late-phase long-term potentiation in isolated dendrites of rat hippocampal CA1 pyramidal neurones. *J Physiol.* 2005;568: 803–813.
 38. Mayford M, Baranes D, Podsypanina K, Kandel ER. The 3'-untranslated region of CaMKII alpha is a cis-acting signal for the localization and translation of mRNA in dendrites. *Proc Natl Acad Sci U S A.* 1996;93: 13250–13255.
 39. Miller S, Yasuda M, Coats JK, Jones Y, Martone ME, Mayford M. Disruption of dendritic translation of CaMKIIalpha impairs stabilization of synaptic plasticity and memory consolidation. *Neuron.* 2002;36: 507–519.
 40. Bassell GJ, Oleynikov Y, Singer RH. The travels of mRNAs through all cells large and small. *FASEB J.* 1999;13: 447–454.
 41. Martin KC, Ephrussi A. mRNA localization: gene expression in the spatial dimension. *Cell.* 2009;136: 719–730.
 42. Knowles RB, Sabry JH, Martone ME, Deerinck TJ, Ellisman MH, Bassell GJ, et al. Translocation of RNA granules in living neurons. *J Neurosci.* 1996;16: 7812–7820.
 43. Knowles RB, Kosik KS. Neurotrophin-3 signals redistribute RNA in neurons. *Proc Natl Acad Sci U S A.* 1997;94: 14804–14808.
 44. Ostroff LE, Fiala JC, Allwardt B, Harris KM. Polyribosomes redistribute from dendritic shafts into spines with enlarged synapses during LTP in developing rat hippocampal slices. *Neuron.* 2002;35: 535–545.
 45. Barondes SH, Squire LR. Time and the biology of memory. *Clin Neurosurg.* 1972;19: 381–396.
 46. Lau LF, Nathans D. Genes induced by serum growth factors. *Molecular Aspects of Cellular Regulation.* 1991. pp. 257–293.
 47. Greenberg M, Ziff E, Greene L. Stimulation of neuronal acetylcholine receptors induces rapid gene transcription. *Science.* 1986;234: 80–83.
 48. Sheng M, Greenberg ME. The regulation and function of c-fos and other immediate early genes in the nervous system. *Neuron.* 1990;4: 477–485.
 49. Guzowski JF. Insights into immediate-early gene function in hippocampal memory consolidation using antisense oligonucleotide and fluorescent imaging approaches. *Hippocampus.* 2002;12: 86–104.
 50. Goelet P, Castellucci VF, Schacher S, Kandel ER. The long and the short of long–

- term memory—a molecular framework. *Nature*. 1986;322: 419–422.
51. Link W, Konietzko U, Kauselmann G, Krug M, Schwanke B, Frey U, et al. Somatodendritic expression of an immediate early gene is regulated by synaptic activity. *Proc Natl Acad Sci U S A*. 1995;92: 5734–5738.
 52. Lyford GL, Yamagata K, Kaufmann WE, Barnes CA, Sanders LK, Copeland NG, et al. Arc, a growth factor and activity-regulated gene, encodes a novel cytoskeleton-associated protein that is enriched in neuronal dendrites. *Neuron*. 1995;14: 433–445.
 53. Guzowski JF, Lyford GL, Stevenson GD, Houston FP, McLaughlin JL, Worley PF, et al. Inhibition of activity-dependent arc protein expression in the rat hippocampus impairs the maintenance of long-term potentiation and the consolidation of long-term memory. *J Neurosci*. 2000;20: 3993–4001.
 54. Paratore S, Alessi E, Coffa S, Torrisi A, Mastrobuono F, Cavallaro S. Early genomics of learning and memory: a review. *Genes Brain Behav*. 2006;5: 209–221.
 55. Cavallaro S, D'Agata V, Manickam P, Dufour F, Alkon DL. Memory-specific temporal profiles of gene expression in the hippocampus. *Proc Natl Acad Sci U S A*. 2002;99: 16279–16284.
 56. Cavallaro S, Schreurs BG, Zhao W, D'Agata V, Alkon DL. Gene expression profiles during long-term memory consolidation. *Eur J Neurosci*. 2001;13: 1809–1815.
 57. D'Agata V, Cavallaro S. Hippocampal gene expression profiles in passive avoidance conditioning. *Eur J Neurosci*. 2003;18: 2835–2841.
 58. Dubnau J, Chiang A-S, Grady L, Barditch J, Gossweiler S, McNeil J, et al. The staufen/pumilio Pathway Is Involved in Drosophila Long-Term Memory. *Curr Biol*. 2003;13: 286–296.
 59. Leil TA, Ossadtchi A, Nichols TE, Leahy RM, Smith DJ. Genes regulated by learning in the hippocampus. *J Neurosci Res*. 2003;71: 763–768.
 60. Luo Y, Long JM, Spangler EL, Longo DL, Ingram DK, Weng NP. Identification of maze learning-associated genes in rat hippocampus by cDNA microarray. *J Mol Neurosci*. 2001;17: 397–404.
 61. Wang Z, Gerstein M, Snyder M. RNA-Seq: a revolutionary tool for transcriptomics. *Nat Rev Genet*. 2009;10: 57–63.
 62. Wang ET, Sandberg R, Luo S, Khrebtkova I, Zhang L, Mayr C, et al. Alternative isoform regulation in human tissue transcriptomes. *Nature*. 2008;456: 470–476.
 63. Sakers K, Lake AM, Khazanchi R, Ouwenga R, Vasek MJ, Dani A, et al. Astrocytes locally translate transcripts in their peripheral processes. *Proc Natl Acad Sci U S A*. 2017;114: E3830–E3838.
 64. Maier T, Güell M, Serrano L. Correlation of mRNA and protein in complex biological samples. *FEBS Lett*. 2009;583: 3966–3973.
 65. Gygi SP, Rochon Y, Robert Franza B, Aebersold R. Correlation between Protein and mRNA Abundance in Yeast. *Mol Cell Biol*. 1999;19: 1720–1730.
 66. Futcher B, Latter GI, Monardo P, McLaughlin CS, Garrels JI. A Sampling of the Yeast Proteome. *Mol Cell Biol*. 1999;19: 7357–7368.
 67. Tian Q, Stepaniants SB, Mao M, Weng L, Feetham MC, Doyle MJ, et al. Integrated Genomic and Proteomic Analyses of Gene Expression in Mammalian Cells. *Mol*

- Cell Proteomics. 2004;3: 960–969.
68. Emmert-Buck MR, Bonner RF, Smith PD, Chuaqui RF, Zhuang Z, Goldstein SR, et al. Laser capture microdissection. *Science*. 1996;274: 998–1001.
 69. Feldman MY. Reactions of nucleic acids and nucleoproteins with formaldehyde. *Prog Nucleic Acid Res Mol Biol*. 1973;13: 1–49.
 70. van den Brink SC, Sage F, Vértesy Á, Spanjaard B, Peterson-Maduro J, Baron CS, et al. Single-cell sequencing reveals dissociation-induced gene expression in tissue subpopulations. *Nat Methods*. 2017;14: 935–936.
 71. King HA, Gerber AP. Translatome profiling: methods for genome-scale analysis of mRNA translation. *Brief Funct Genomics*. 2016;15: 22–31.
 72. Ingolia NT, Ghaemmaghami S, Newman JRS, Weissman JS. Genome-wide analysis in vivo of translation with nucleotide resolution using ribosome profiling. *Science*. 2009;324: 218–223.
 73. Heiman M, Schaefer A, Gong S, Peterson JD, Day M, Ramsey KE, et al. A Translational Profiling Approach for the Molecular Characterization of CNS Cell Types. *Cell*. 2008;135: 738–748.
 74. Ainsley JA, Drane L, Jacobs J, Kittelberger KA, Reijmers LG. Functionally diverse dendritic mRNAs rapidly associate with ribosomes following a novel experience. *Nat Commun*. 2014;5: 4510.
 75. Drane L, Ainsley JA, Mayford MR, Reijmers LG. A transgenic mouse line for collecting ribosome-bound mRNA using the tetracycline transactivator system. *Front Mol Neurosci*. 2014;7: 82.
 76. Cook-Snyder DR, Jones A, Reijmers LG. A retrograde adeno-associated virus for collecting ribosome-bound mRNA from anatomically defined projection neurons. *Front Mol Neurosci*. 2015;8: 56.
 77. Richter JD, Collier J. Pausing on Polyribosomes: Make Way for Elongation in Translational Control. *Cell*. 2015;163: 292–300.
 78. Cajigas IJ, Tushev G, Will TJ, tom Dieck S, Fuerst N, Schuman EM. The local transcriptome in the synaptic neuropil revealed by deep sequencing and high-resolution imaging. *Neuron*. 2012;74: 453–466.
 79. Cho J, Yu N-K, Choi J-H, Sim S-E, Kang SJ, Kwak C, et al. Multiple repressive mechanisms in the hippocampus during memory formation. *Science*. 2015;350: 82–87.
 80. Chen PB, Kawaguchi R, Blum C, Achiro JM, Coppola G, O’Dell TJ, et al. Mapping Gene Expression in Excitatory Neurons during Hippocampal Late-Phase Long-Term Potentiation. *Front Mol Neurosci*. 2017;10: 39.
 81. Doyle JP, Dougherty JD, Heiman M, Schmidt EF, Stevens TR, Ma G, et al. Application of a translational profiling approach for the comparative analysis of CNS cell types. *Cell*. 2008;135: 749–762.
 82. Heiman M, Kulicke R, Fenster RJ, Greengard P, Heintz N. Cell type-specific mRNA purification by translating ribosome affinity purification (TRAP). *Nat Protoc*. 2014;9: 1282–1291.
 83. Dobin A, Davis CA, Schlesinger F, Drenkow J, Zaleski C, Jha S, et al. STAR:

- ultrafast universal RNA-seq aligner. *Bioinformatics*. 2013;29: 15–21.
84. Anders S, Pyl PT, Huber W. HTSeq - A Python framework to work with high-throughput sequencing data [Internet]. 2014. doi:10.1101/002824
 85. Anders S, Anders S, Huber W. Differential expression analysis for sequence count data. *Nature Precedings*. 2010; doi:10.1038/npre.2010.4282.1
 86. Mudge JM, Harrow J. Creating reference gene annotation for the mouse C57BL6/J genome assembly. *Mamm Genome*. 2015;26: 366–378.
 87. Huang DW, Sherman BT, Lempicki RA. Systematic and integrative analysis of large gene lists using DAVID bioinformatics resources. *Nat Protoc*. 2009;4: 44–57.
 88. Huang DW, Sherman BT, Lempicki RA. Bioinformatics enrichment tools: paths toward the comprehensive functional analysis of large gene lists. *Nucleic Acids Res*. 2009;37: 1–13.
 89. Love MI, Huber W, Anders S. Moderated estimation of fold change and dispersion for RNA-seq data with DESeq2. *Genome Biol*. 2014;15: 550.
 90. Zhong J, Zhang T, Bloch LM. Dendritic mRNAs encode diversified functionalities in hippocampal pyramidal neurons. *BMC Neurosci*. 2006;7: 17.
 91. Mayford M, Bach ME, Huang YY, Wang L, Hawkins RD, Kandel ER. Control of memory formation through regulated expression of a CaMKII transgene. *Science*. 1996;274: 1678–1683.
 92. Guzowski JF, McNaughton BL, Barnes CA, Worley PF. Environment-specific expression of the immediate-early gene *Arc* in hippocampal neuronal ensembles. *Nat Neurosci*. 1999;2: 1120–1124.
 93. Lightfoot S, Salowsky R, Buhlmann C. RNA integrity number: towards standardization of RNA quality assessment for better reproducibility and reliability of gene expression experiments. *Breast Cancer Res*. 2005;7. doi:10.1186/bcr1197
 94. Zeisel A, Muñoz-Manchado AB, Codeluppi S, Lönnerberg P, La Manno G, Juréus A, et al. Brain structure. Cell types in the mouse cortex and hippocampus revealed by single-cell RNA-seq. *Science*. 2015;347: 1138–1142.
 95. Kosik KS. Life at Low Copy Number: How Dendrites Manage with So Few mRNAs. *Neuron*. 2016;92: 1168–1180.
 96. Wang L, Yi R. 3'UTRs take a long shot in the brain. *Bioessays*. 2013;36: 39–45.
 97. Miura P, Shenker S, Andreu-Agullo C, Westholm JO, Lai EC. Widespread and extensive lengthening of 3' UTRs in the mammalian brain. *Genome Res*. 2013;23: 812–825.
 98. Tian B, Manley JL. Alternative cleavage and polyadenylation: the long and short of it. *Trends Biochem Sci*. 2013;38: 312–320.
 99. An JJ, Gharami K, Liao G-Y, Woo NH, Lau AG, Vanevski F, et al. Distinct Role of Long 3' UTR BDNF mRNA in Spine Morphology and Synaptic Plasticity in Hippocampal Neurons. *Cell*. 2008;134: 175–187.
 100. Dictenberg JB, Swanger SA, Antar LN, Singer RH, Bassell GJ. A direct role for FMRP in activity-dependent dendritic mRNA transport links filopodial-spine morphogenesis to fragile X syndrome. *Dev Cell*. 2008;14: 926–939.
 101. Kao D-I, Aldridge GM, Weiler IJ, Greenough WT. Altered mRNA transport,

- docking, and protein translation in neurons lacking fragile X mental retardation protein. *Proc Natl Acad Sci U S A*. 2010;107: 15601–15606.
102. Smith LN, Jedynak JP, Fontenot MR, Hale CF, Dietz KC, Taniguchi M, et al. Fragile X mental retardation protein regulates synaptic and behavioral plasticity to repeated cocaine administration. *Neuron*. 2014;82: 645–658.
 103. Darnell JC, Van Driesche SJ, Zhang C, Hung KY, Mele A, Fraser CE, et al. FMRP stalls ribosomal translocation on mRNAs linked to synaptic function and autism. *Cell*. 2011;146: 247–261.
 104. de Wit J, Hong W, Luo L, Ghosh A. Role of leucine-rich repeat proteins in the development and function of neural circuits. *Annu Rev Cell Dev Biol*. 2011;27: 697–729.
 105. Eberwine J, Belt B, Kacharina JE, Miyashiro K. Analysis of subcellularly localized mRNAs using in situ hybridization, mRNA amplification, and expression profiling. *Neurochem Res*. 2002;27: 1065–1077.
 106. Heyer EE, Moore MJ. Redefining the Translational Status of 80S Monosomes. *Cell*. 2016;164: 757–769.
 107. Ascoli GA, Donohue DE, Halavi M. NeuroMorpho.Org: a central resource for neuronal morphologies. *J Neurosci*. 2007;27: 9247–9251.
 108. Macaulay IC, Voet T. Single cell genomics: advances and future perspectives. *PLoS Genet*. 2014;10: e1004126.
 109. Islam S, Kjallquist U, Moliner A, Zajac P, -B. Fan J, Lonnerberg P, et al. Characterization of the single-cell transcriptional landscape by highly multiplex RNA-seq. *Genome Res*. 2011;21: 1160–1167.
 110. Dueck H, Khaladkar M, Kim TK, Spaethling JM, Francis C, Suresh S, et al. Deep sequencing reveals cell-type-specific patterns of single-cell transcriptome variation. *Genome Biol*. 2015;16: 122.
 111. Middleton SA, Eberwine J, Kim J. Comprehensive catalog of dendritically localized mRNA isoforms from sub-cellular sequencing of single mouse neurons [Internet]. 2018. doi:10.1101/278648
 112. Frey U, Morris RG. Synaptic tagging and long-term potentiation. *Nature*. 1997;385: 533–536.
 113. Redondo RL, Morris RGM. Making memories last: the synaptic tagging and capture hypothesis. *Nat Rev Neurosci*. 2011;12: 17–30.
 114. Tanaka J-I, Horiike Y, Matsuzaki M, Miyazaki T, Ellis-Davies GCR, Kasai H. Protein synthesis and neurotrophin-dependent structural plasticity of single dendritic spines. *Science*. 2008;319: 1683–1687.
 115. Bosch M, Castro J, Saneyoshi T, Matsuno H, Sur M, Hayashi Y. Structural and Molecular Remodeling of Dendritic Spine Substructures during Long-Term Potentiation. *Neuron*. 2014;82: 444–459.
 116. Choi J-H, Sim S-E, Kim J-I, Choi DI, Oh J, Ye S, et al. Interregional synaptic maps among engram cells underlie memory formation. *Science*. 2018;360: 430–435.
 117. Vicario A, Colliva A, Ratti A, Davidovic L, Baj G, Gricman L, et al. Dendritic targeting of short and long 3' UTR BDNF mRNA is regulated by BDNF or NT-3

- and distinct sets of RNA-binding proteins. *Front Mol Neurosci.* 2015;8: 62.
118. Kobayashi H, Yamamoto S, Maruo T, Murakami F. Identification of a cis-acting element required for dendritic targeting of activity-regulated cytoskeleton-associated protein mRNA. *Eur J Neurosci.* 2005;22: 2977–2984.
 119. Blichenberg A, Schwanke B, Rehbein M, Garner CC, Richter D, Kindler S. Identification of a cis-acting dendritic targeting element in MAP2 mRNAs. *J Neurosci.* 1999;19: 8818–8829.
 120. Böckers TM, Segger-Junius M, Iglauer P, Bockmann J, Gundelfinger ED, Kreutz MR, et al. Differential expression and dendritic transcript localization of Shank family members: identification of a dendritic targeting element in the 3' untranslated region of Shank1 mRNA. *Mol Cell Neurosci.* 2004;26: 182–190.
 121. Moccia R, Chen D, Lyles V, Kapuya E, E Y, Kalachikov S, et al. An unbiased cDNA library prepared from isolated *Aplysia* sensory neuron processes is enriched for cytoskeletal and translational mRNAs. *J Neurosci.* 2003;23: 9409–9417.
 122. Puthanveetil SV, Antonov I, Kalachikov S, Rajasethupathy P, Choi Y-B, Kohn AB, et al. A strategy to capture and characterize the synaptic transcriptome. *Proc Natl Acad Sci U S A.* 2013;110: 7464–7469.
 123. Graber TE, McCamphill PK, Sossin WS. A recollection of mTOR signaling in learning and memory. *Learn Mem.* 2013;20: 518–530.
 124. Zhou X, Liao W-J, Liao J-M, Liao P, Lu H. Ribosomal proteins: functions beyond the ribosome. *J Mol Cell Biol.* 2015;7: 92–104.
 125. Daftuar L, Zhu Y, Jacq X, Prives C. Ribosomal proteins RPL37, RPS15 and RPS20 regulate the Mdm2-p53-MdmX network. *PLoS One.* 2013;8: e68667.
 126. Mattson MP, Duan W. “Apoptotic” biochemical cascades in synaptic compartments: Roles in adaptive plasticity and neurodegenerative disorders. *J Neurosci Res.* 1999;58: 152–166.
 127. Santoro MR, Bray SM, Warren ST. Molecular mechanisms of fragile X syndrome: a twenty-year perspective. *Annu Rev Pathol.* 2012;7: 219–245.
 128. Lai K-O, Ip NY. Structural plasticity of dendritic spines: the underlying mechanisms and its dysregulation in brain disorders. *Biochim Biophys Acta.* 2013;1832: 2257–2263.
 129. Chen E, Sharma MR, Shi X, Agrawal RK, Joseph S. Fragile X mental retardation protein regulates translation by binding directly to the ribosome. *Mol Cell.* 2014;54: 407–417.
 130. Steward O, Bakker CE, Willems PJ, Oostra BA. No evidence for disruption of normal patterns of mRNA localization in dendrites or dendritic transport of recently synthesized mRNA in FMR1 knockout mice, a model for human fragile-X mental retardation syndrome. *Neuroreport.* 1998;9: 477–481.
 131. Bambah-Mukku D, Travaglia A, Chen DY, Pollonini G, Alberini CM. A Positive Autoregulatory BDNF Feedback Loop via C/EBP Mediates Hippocampal Memory Consolidation. *Journal of Neuroscience.* 2014;34: 12547–12559.
 132. Bekinschtein P, Cammarota M, Izquierdo LM, Bevilaqua LRM, Izquierdo I, Medina JH. Persistence of long-term memory storage requires a late protein synthesis- and

- BDNF- dependent phase in the hippocampus. *Neuron*. 2007;53: 261–277.
133. Dehorter N, Ciceri G, Bartolini G, Lim L, del Pino I, Marín O. Tuning of fast-spiking interneuron properties by an activity-dependent transcriptional switch. *Science*. 2015;349: 1216–1220.
 134. Chotiner JK, Khorasani H, Nairn AC, O’Dell TJ, Watson JB. Adenylyl cyclase-dependent form of chemical long-term potentiation triggers translational regulation at the elongation step. *Neuroscience*. 2003;116: 743–752.
 135. Izquierdo I. Role of NMDA receptors in memory. *Trends Pharmacol Sci*. 1991;12: 128–129.
 136. Tang YP, Wang H, Feng R, Kyin M, Tsien JZ. Differential effects of enrichment on learning and memory function in NR2B transgenic mice. *Neuropharmacology*. 2001;41: 779–790.
 137. Rowland LM, Astur RS, Jung RE, Bustillo JR, Lauriello J, Yeo RA. Selective cognitive impairments associated with NMDA receptor blockade in humans. *Neuropsychopharmacology*. 2005;30: 633–639.
 138. Rezvani AH. Involvement of the NMDA System in Learning and Memory. In: Levin ED, Buccafusco JJ, editors. *Animal Models of Cognitive Impairment*. Boca Raton (FL): CRC Press/Taylor & Francis; 2011.
 139. Igaz LM, Vianna MRM, Medina JH, Izquierdo I. Two time periods of hippocampal mRNA synthesis are required for memory consolidation of fear-motivated learning. *J Neurosci*. 2002;22: 6781–6789.
 140. Banno T, Kohno K. Conformational changes of the smooth endoplasmic reticulum are facilitated by L-glutamate and its receptors in rat Purkinje cells. *J Comp Neurol*. 1998;402: 252–263.
 141. Ramírez OA, Couve A. The endoplasmic reticulum and protein trafficking in dendrites and axons. *Trends Cell Biol*. 2011;21: 219–227.
 142. Bahrami S, Drabløs F. Gene regulation in the immediate-early response process. *Adv Biol Regul*. 2016;62: 37–49.
 143. Siddiqui TJ, Tari PK, Connor SA, Zhang P, Dobie FA, She K, et al. An LRRTM4-HSPG complex mediates excitatory synapse development on dentate gyrus granule cells. *Neuron*. 2013;79: 680–695.
 144. Kittler JT, Lorena Arancibia-Carcamo I, Moss SJ. Association of GRIP1 with a GABAA receptor associated protein suggests a role for GRIP1 at inhibitory synapses. *Biochem Pharmacol*. 2004;68: 1649–1654.
 145. Misgeld T, Kummer TT, Lichtman JW, Sanes JR. Agrin promotes synaptic differentiation by counteracting an inhibitory effect of neurotransmitter. *Proc Natl Acad Sci U S A*. 2005;102: 11088–11093.
 146. Buckley PT, Lee MT, Sul J-Y, Miyashiro KY, Bell TJ, Fisher SA, et al. Cytoplasmic intron sequence-retaining transcripts can be dendritically targeted via ID element retrotransposons. *Neuron*. 2011;69: 877–884.
 147. Sharangdhar T, Sugimoto Y, Heraud-Farlow J, Fernández-Moya SM, Ehses J, Ruiz de Los Mozos I, et al. A retained intron in the 3’-UTR of mRNA mediates its Staufen2- and activity-dependent localization to neuronal dendrites. *EMBO Rep*.

2017;18: 1762–1774.

148. Wu B, Eliscovich C, Yoon YJ, Singer RH. Translation dynamics of single mRNAs in live cells and neurons. *Science*. 2016;352: 1430–1435.